ORGANOMETALLICS

Article

Cite This: *Organometallics* XXXX, XXX, XXX–XXX

Iridacycles as Catalysts for the Autotandem Conversion of Nitriles into Amines by Hydrosilylation: Experimental Investigation and Scope

Mustapha Hamdaoui, Camille Desrousseaux, Houda Habbita, and Jean-Pierre Djukic*

Institut de Chimie de Strasbourg, UMR 7177 CNRS, Université de Strasbourg, 4 rue Blaise Pascal, F-67000 Strasbourg, France

Supporting Information

ABSTRACT: The set of iridacycles [{C,N}Cp*Ir^{III}-Cl] ({C,N} = benzo[*h*]quinoline, dibenzo[*f*,*h*]quinoline) containing the (pentamethylcyclopentadienyl)iridium(III) unit were synthesized and derivatized into cations [{C,N}Cp*Ir-NCMe]$^+$ associated with BArF-type anions. The latter salts were benchmarked for their potential catalytic properties toward $HSiEt_3$ in a H_2-releasing test reaction. The best-performing BArF-type salts demonstrated the capability to promote with a low catalytic load of ca. 0.5−1 mol % the autotandem hydrosilylation of acetonitrile, propionitrile, and a series of arylnitrile substrates. Mechanistic investigations confirmed the preliminary formation of a silane−iridacycle adduct by electrophilic and heterolytic activation of the Si−H bond. The molecular structure of a new example of such an adduct was resolved by X-ray diffraction analysis. Theoretical considerations support a donor−acceptor [{C,N}Cp*Ir^{III}-H]→[$SiEt_3$]$^+$ ({C,N} = benzo[*h*]quinolinyl) formulation where the cationic silyl moiety acting as a *Z* ligand binds both Ir and H centers. Under the conditions of the catalysis, the latter adduct is assumed to transfer readily the electrophilic [$SiEt_3$]$^+$ moiety to the nucleophilic nitrile substrate to form a *N*-silylnitrilium cation and the neutral [{C,N}Cp*Ir-H]. The latter reduces the *N*-silylnitrilium into the corresponding *N*-silylimine, which undergoes further *N*-silylation and reduction to yield the final *N*,*N*-disilylamine. Under optimal conditions of low catalyst load (70 °C, 0.5 mol %) the autotandem hydrosilylation of arylnitriles produces the silylated amines in yields >80% in 24 h.

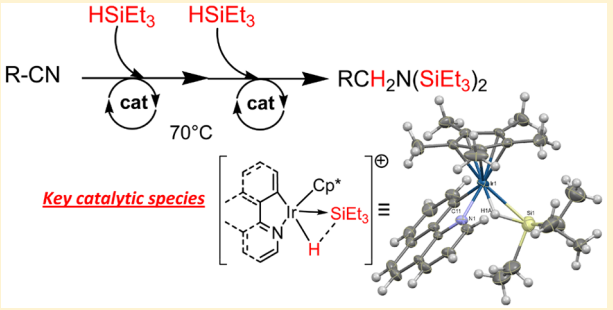

INTRODUCTION

The catalytic reduction of nitriles is a highly valuable[1] reaction, and mild as well as selective methods of reduction to either imines or amines are rare.[2] Although alkyl- and arylnitriles can be reduced stoichiometrically with alumino- and borohydrides[3] or catalytically hydrogenated with H_2,[4] the lack of selectivity associated with high potential hazards are prohibitive obstacles to industrial scale-up. Therefore, catalyzed hydrosilylations of nitriles into *N*,*N*-bis(silyl)amines with minimized operational risks are particularly sought. If one relies on the few studies published in the field, mild and selective catalytic hydrosilylation of nitriles might be considered as a rather difficult transformation to achieve. The main difficulty seemingly arises from the strong C≡N bond (bond dissociation energy 179.3 kcal/mol, 750.0 kJ/mol)[5] and from the moderate electrophilic character of the sp carbon. In 1961, Calas et al. reported the first transition-metal-based catalytic hydrosilylation of nitriles using $ZnCl_2$.[6] Other studies that followed this seminal report successfully applied cobalt-,[7] rhenium-,[8] rhodium-,[9] ruthenium-,[10] and zinc-based[11] complexes as precatalysts. However, in most cases heating at 100 °C combined with high catalyst loadings was necessary to achieve a rather limited substrate scope and selectivity. Significant improvement in the autotandem double hydrosilylation of nitriles was achieved by using, for example, ruthenium-based (Scheme 1)[10,12] and iron-based[13] organometallic catalysts. Other systems based on main-group metals and fluoride salts were also found to catalyze this transformation.[14−16]

To the best of our knowledge, the hydrosilylation of nitriles catalyzed by iridium complexes has not yet been reported. The only barely related study was reported by Bergman et al. in 2002.[17] In the present article, we report on the capability of readily accessible Cp*Ir-based iridacycles to promote the double hydrosilylation of a series of nitrile group containing organic substrates following a so-called autotandem[13,19] catalyzed process. This report is a continuation of our effort to develop the use of such iridacycles as potential catalysts of "one-pot" autotandem[18] reactions.[19] This endeavor has widened the field of organic reactions that could be catalyzed by various formulations of the iridacyclic catalysts, which consist of either the neutral chlorido or cationic solvato complexes.[20] All have shown outstanding performance in the transformation of imines, alkynes, alcohols, acetals, and amides and other carbonyl-containing compounds.[20] In a recent report, we disclosed the peculiar mode of activation of $HSiEt_3$ by a cationic iridacycle.[19b] It was shown that the reaction of a solvato iridacycle with $HSiEt_3$ mainly led to the formation of a

Received: October 9, 2017

DOI: 10.1021/acs.organomet.7b00749
Organometallics XXXX, XXX, XXX–XXX

Scheme 1. Chosen Examples of Early Studies on the Hydrosilylation of Benzonitrile Catalyzed by Transition-Metal Complexes

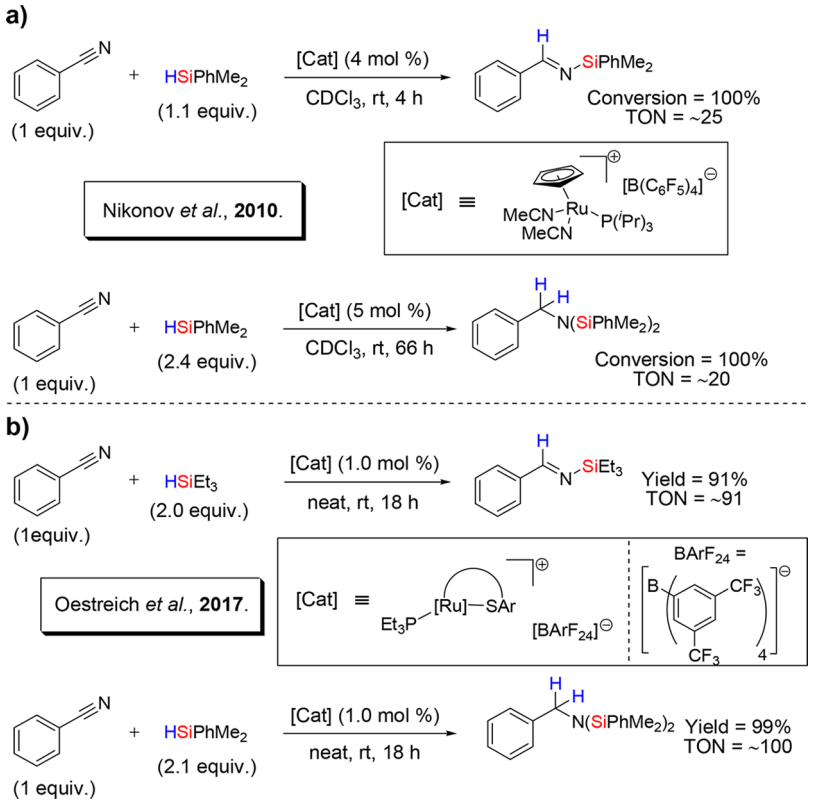

new adduct in which the Ir-bound silyl group had the properties of a *Z*-type silylium ligand rather than that of a *X*-type silyl ligand, according to Green's ligand class[21] formalism.[22] This led us to propose that any catalysis which ensues should follow a heterolytic pathway where the activation of silane operates by the concerted transfer of a hydride from the silane to the iridium center combined with the capture of the silylium moiety: this mechanism relates to the concept of "electrophilic activation" outlined by Tilley et al.[23] in a recent review. In the present report a highly active iridacyclic precatalyst is identified, which displays excellent capability to promote the autotandem double hydrosilylation of a variety of nitrile-containing substrates as well as the hydrosilylation of carbonyl-containing substrates, which is considered here as a reference reaction.

RESULTS AND DISCUSSION

Synthesis and Structural Characterization of New Precatalysts. To address the capabilities of iridacycles in promoting the hydrosilylation of nitriles, we chose to synthesize a few new precatalysts differing either in the nature of the {C,N} chelating ligand or in the nature of the counteranion X, assuming that slight backbone variation and proper choice of anion could lead to an optimal catalyst. The synthesis of the chlorido-bound iridacycles (Scheme 2) was performed by applying a standard procedure consisting of stirring a mixture of ligands **1a−c**,[24] NaOAc, and $[Ir(\mu\text{-Cl})ClCp^*]_2$[25] in CH_2Cl_2 at room temperature for over 16 h, affording complexes **2a−c** with yields of between 60% (**2c**) and 94%. Complexes **2a−c** were subsequently all converted into acetonitrile solvato salts **3a−c** by the chlorido-abstraction procedures described earlier that use as a driving force the precipitation of either NaCl (sodium tetraarylborates) or AgCl (AgOTf).[19b] As shown

Scheme 2. Synthesis of Precatalysts [3a−c][X] by Cycloiridation of 2-Phenylpyridine (1a), Benzo[*h*]quinoline (1b), and Dibenzo[*f*,*h*]quinoline (1c) Followed by Chloride Abstraction and Replacement by Coordinated Acetonitrile

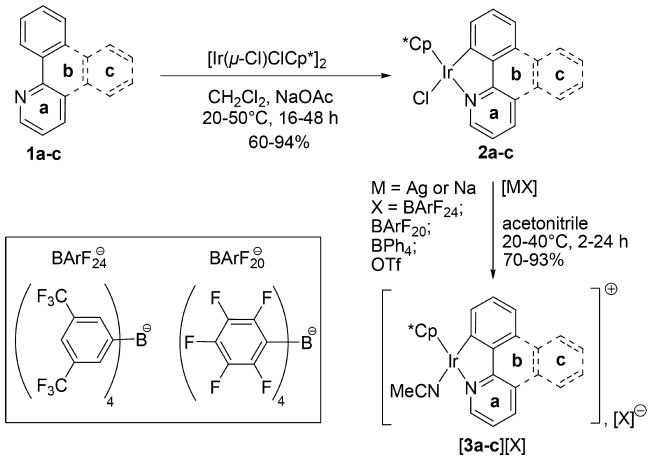

below, only cation $[\mathbf{3b}]^+$ was prepared associated with the counteranions OTf, BPh_4, $BArF_{20}$, and $BArF_{24}$ for the purpose of comparing the possible effect of the anion on the catalytic performance. Cation $[\mathbf{3a}]^+$ was associated with $BArF_{20}$ and $BArF_{24}$, whereas $[\mathbf{3c}]^+$ was only associated with $BArF_{24}$. All new complexes were characterized analytically and spectroscopically by conventional methods.

^1H and ^{13}C NMR spectra (recorded in CD_2Cl_2 at 298 K, unless otherwise stated) of all the ionic iridiacycles disclosed in this paper showed that the chemical shifts of the NCMe ligand can slightly vary with the nature of the {C,N} ligand and of the counteranion X (Table 1). The case of $[\mathbf{3b}][BPh_4]$ deviates

DOI: 10.1021/acs.organomet.7b00749
Organometallics XXXX, XXX, XXX−XXX

Table 1. Selected Solution ^{1}H and ^{13}C NMR Chemical Shifts of Ionic Iridacycles[a]

	δ (ppm) of [Ir]-NC*Me*			δ (ppm) of [Ir]-C_5Me_5		
		^{13}C			^{13}C	
compound	^{1}H	NC	*Me*	^{1}H	C_5	Me_5
[**3a**][$BArF_{24}$]	2.23	118.3	4.2	1.62	91.8	8.9
[**3a**][$BArF_{20}$]	2.27	118.4	4.3	1.68	91.8	8.9
[**3b**][$BArF_{24}$]	2.12	118.5	4.2	1.73	91.6	9.1
[**3b**][$BArF_{20}$]	2.15	119.0	4.6	1.75	92.1	9.6
[**3b**][BPh_4]	1.59	119.0	3.4	1.74	91.5	9.2
[**3b**][OTf]	2.28	119.0	4.1	1.79	91.1	9.0
[**3c**][$BArF_{24}$][b]	2.41	118.3	3.4	1.86	92.3	10.0

[a]Recorded in CD_2Cl_2 (unless otherwise stated) at 298 K. [b]In d_6-acetone.

from the general trend, for the methyl ^{1}H and ^{13}C nuclei of the metal-bound NCMe resonate at higher field in comparison to other salts (^{1}H, ∼2.2 ppm; ^{13}C, ∼4.1 ppm), i.e. at respectively 1.59 and 3.4 ppm. Single-crystal X-ray diffraction analyses produced the molecular structures of salts [**3a**][$BArF_{20}$], [**3b**][BPh_4], [**3b**][$BArF_{20}$], [**3b**][$BArF_{24}$], and [**3c**][$BArF_{24}$] (cf. the Supporting Information and CIF files). For the sake of conciseness only the structures of [**3b**][$BArF_{24}$] and [**3c**]-[$BArF_{24}$] are displayed in Figure 1 (cf. the Supporting Information and CIF files). The structures did not reveal any significant variations of distances that could be related to any possible electronic effect induced by the change of {C,N} chelating ligand on going from **3a** to the polyaromatic **3b** and **3c**. For instance, the Ir−N(MeCN) bond distance was found to be invariant within the limits imposed by estimated standard deviations. Quite interestingly, the shortest distance of separation between the Ir atom of the cation and the B atom of the counteranion in the crystal lattice of all investigated complexes was found to remain at around 7.4 Å. For salts of [**3b**]$^+$ this distance was found to slightly increase from 7.315(4) to 7.411(2) and 7.617(2) Å on going from [**3b**][BPh_4] to [**3b**][$BArF_{20}$] and [**3b**][$BArF_{24}$], which might be related to the increase in the steric volume of the anion.

Furthermore, a close analysis of the ^{1}H NMR spectrum of a pure sample of [**3b**][BPh_4] left to stand in solution (CD_2Cl_2) at room temperature for less than 1 h revealed the presence of several new signals assigned to the products of decomposition of [**3b**][BPh_4]. One of the products was unambigously identified to be free benzene (singlet at 7.36 ppm;[26] ratio [**3b**][BPh_4]:benzene ≈ 1:0.2), suggesting the cleavage of the C−B bond of one of the four phenyls of the $[BPh_4]^-$ anion. Other untraceable product(s) were distinguishable from weak signals appearing at 7.45 (t, 6H relative to benzene) and 7.61 ppm (m, 6H relative to benzene). It is worth noting that free NCMe could also be detected (broad singlet at 1.97 ppm, 3H relative to benzene).

Benchmark of Iridacyclic Precatalysts. In a previous report,[19b] we presented a straightforward setup for the qualitative evaluation of the performance of iridacyclic catalysts in the dehydrosilylation of alcohols by silanes. This reaction, which releases a significant amount of dihydrogen gas within a few seconds, was carried out in a thermo-regulated sealed glass reactor and monitored by piezometry. In the typical experimental setup (cf. Scheme S1 in the Supporting Information) the variation of internal reactor pressure caused by the release of H_2[19] in the overhead volume above the

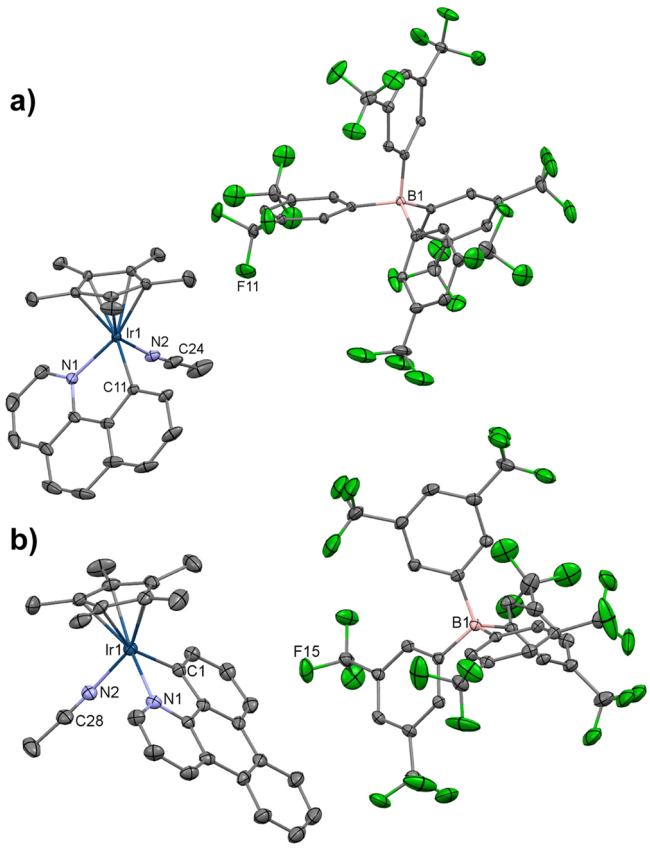

Figure 1. ORTEP-type (thermal ellipsoid) drawings of the molecular structures of [**3b**][$BArF_{24}$] (a) and [**3c**][$BArF_{24}$] (b) drawn at the 30% probability level. Hydrogen atoms and solvent molecules are omitted for the sake of clarity. F atoms were found with a 50% positional disorder at some CF_3 groups: only one position was retained in this graphical representation (cf. the CIF files for details). Selected interatomic distances (Å) and angle (deg) for [**3b**][$BArF_{24}$]: C11−Ir1 2.073(3), N1−Ir1 2.099(3), N2−Ir1 2.034(3), C24−N2 1.153(5), C11−Ir1−N1 79.15(12) . Selected interatomic distances (Å) and angle (deg) for [**3c**][$BArF_{24}$]: C1−Ir1 2.051(5), N1−Ir1 2.107(4), N2−Ir1 2.061(4), C1−Ir1−N1 78.23(18).

reaction solution is captured at high sampling rates by an adequately chosen absolute pressure−voltage linear transducer interfaced to an analog−logic converter and a computer. Since reproducible determinations of kinetic parameters were achieved, this setup was used for precatalyst discovery. Indeed, the fact that catalyzed *O*-dehydrosilylation of alcohols and hydrosilylation of carbonyls, imines, etc. were assumed to involve common key silane activation steps and intermediates, this setup could potentially help identifying the most promising precatalysts for the challenging duty of achieving the hydrosilylation of nitriles.

Therefore, our efforts mainly focused on the evaluation of BArF-based ($BArF_{20}$ and $BArF_{24}$) salts, knowing that they generally produce the highest catalytic activity for this reaction.[19b] Table 2 gathers the main results collected for the comparative evaluation of five precatalyst salts: i.e., [**3a**]-[$BArF_{20}$], [**3b**][$BArF_{20}$], [**3a**][$BArF_{24}$], [**3b**][$BArF_{24}$], and [**3c**][$BArF_{24}$]. Triethylsilane was favored here, for it gave the fastest reactions and the highest conversions in comparison to other considered silanes.

Entries 1−5 in Table 2 give experiments carried out using a 1:1 ratio of benzyl alcohol and triethylsilane (eq 1), whereas

DOI: 10.1021/acs.organomet.7b00749
Organometallics XXXX, XXX, XXX−XXX

Table 2. Benchmark of BArF Salts of Iridacycles $[3a–c]^+$ through *O*-Silylation of Benzyl Alcohol at 20 °C

entry	precatalyst (amt (μmol))	t (s)	yield[a] (%)	v_i[b] (esd) (10^{-2} M s^{-1})	TON[c] (%)	TOF_t[d] (h^{-1})
1[e]	[**3a**][$BArF_{20}$] (4.8)	37	81	13.2(3)	812	0.08 × 10^6
2[e]	[**3b**][$BArF_{20}$] (4.8)	1.6	100	57(5)	1002	2 0.2 × 10^6
3[e]	[**3a**][$BArF_{24}$] (5.0)	34	85	10(1)	818	0.09 × 10^6
4[e]	[**3b**][$BArF_{24}$] (4.4)	1.4	100	42(9)	1093	2.9 × 10^6
5[e]	[**3c**][$BArF_{24}$] (4.8)	2.3	100	42(2)	1002	1.6 × 10^6
6[f]	[**3a**][$BArF_{24}$] (4.8)	16	100	8(6)	1002	0.2 × 10^6
7[f]	[**3b**][$BArF_{24}$] (4.4)	2.5	100	40(2)	1093	1.6 × 10^6

[a]Yield in evolved H_2. [b]initial rate $v_i = -(d[Et_3SiH]/dt)_i$ inferred from the rate of H_2 gas release. [c]TON: turnover number, calculated at the highest conversion as the molar ratio of inferred silylated alcohol/initial precatalyst. [d]TOF_t: turnover frequency calculated at time t corresponding to the maximum of conversion calculated as the ratio TON/time. [e]Conditions unless specified otherwise: benzyl alcohol (0.50 mL, 4.8 mmol), $HSiEt_3$ (0.8 mL, 5.0 mmol), precatalyst (ca. 0.1 mol %, ca. 5 μmol) in a respective 962:1000:1 ratio in 1,2-dichloroethane (0.5 mL) at 20 ± 0.1 °C. [f]1.9 equiv of benzyl alcohol was used (1 mL, 9.6 mmol): i.e., a respective 1920:1000:1 ratio in 1,2-dichloroethane (0.5 mL) at 20 ± 0.1 °C.

entries 6 and 7 are associated with experiments using a ca. 2:1 benzyl alcohol $HSiEt_3$ ratio.

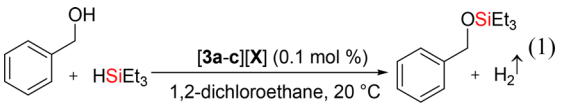

In all cases, data in Table 2 suggest that salts based on $[3a]^+$ are far slower and less efficient in comparison to those based on $[3b]^+$ and $[3c]^+$; the turnover frequencies (TOF_t) are 1 order of magnitude lower for $[3a]^+$. Even though total conversion can be reached over reaction times much longer than those considered in this benchmark procedure, the turnovers for $[3a]^+$ -based salts are 20% lower than for $[3b]^+$- and $[3c]^+$-based precatalysts. The order of catalytic efficiency is $[3b]^+ > [3c]^+ \gg [3a]^+$. Quite stunning is the time required to produce 100% of the expected H_2 gas amount with $[3b]^+$ and $[3c]^+$ salts: less than 3 s after the injection of the $ClCH_2CH_2Cl$ solution of precatalyst in the mixture of benzyl alcohol and $HSiEt_3$.

The short induction period of ca. 1 s noticeable in Figure 2 for almost all cases of precatalysts can be rationalized by the activation step necessary to convert the precatalyst into the active catalyst, which is the silylium-bound hydrido-iridium intermediate $[4]^+$ (eq 2), one example of which was reported previously.[19b] This transformation requires the endoergonic departure of MeCN followed by the activation of $HSiEt_3$ and

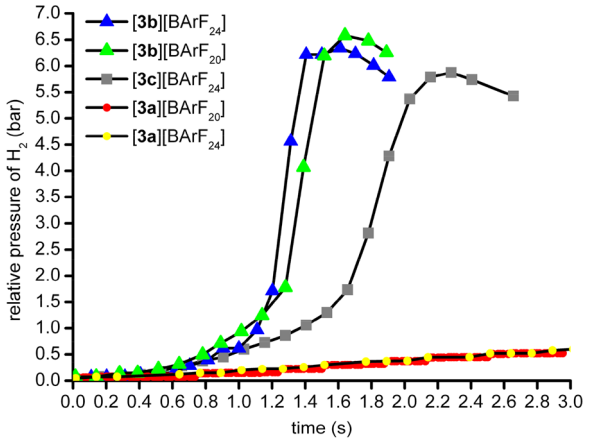

Figure 2. Variation of the relative pressure of hydrogen (bar) vs time (s) in the dehydro-*O*-silylation of benzyl alcohol by $HSiEt_3$ (1:1 ratio) catalyzed by [**3a–c**][X] (X= $BArF_{20}$, $BArF_{24}$).

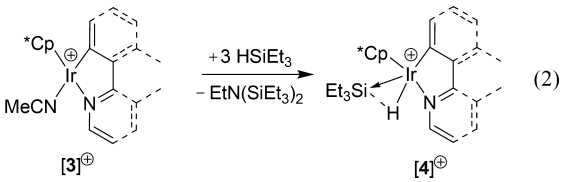

the largely exothermic double hydrosilylation of the released MeCN catalyzed by $[4]^+$ (eq 2).[19b] As far as the effect of BArF counteranions is concerned, Table 2 reveals equal efficiencies for $BArF_{20}$ and $BArF_{24}$ salts: the TOF_t and initial rate v_i values for [**3b**][$BArF_{20}$] and [**3b**][$BArF_{24}$] are of the same magnitude, i.e. around 2.5 × 10^6 h^{-1} and 48 × 10^{-2} M s^{-1}, respectively. Finally, the effect of the alcohol:silane ratio is better evaluated by v_i, which depicts the rate of H_2 gas release in the initiation time period, than by TOF_t. TOF_t, which gives an average estimate of the rate of the catalysis, suggests contradictory conclusions. For [**3b**][$BArF_{24}$], excess alcohol seemingly decreases the TOF_t value by ca. 10^6 h^{-1}, which could be interpreted as a sign of coordinative inhibition of the catalyst by the alcohol. However, the opposite observation is made for [**3a**][$BArF_{24}$], which seemingly increases its TOF_t when a 2:1 alcohol:silane ratio is used. When initial rates v_i are considered instead for both [**3a**][$BArF_{24}$] and [**3b**][$BArF_{24}$], one can notice that the values are, if not constant, only slightly lowered when the amount of alcohol increases, which rather suggests that no coordinative inhibition of the catalysis by the alcohol takes place in the early stages of the catalysis.

In fact, the most important aspect here is that, given the limited amount of $ClCH_2CH_2Cl$ used, the polarity of the solution is mostly governed by the change in composition of the medium as the dehydrosilylation reaction develops. Indeed, the steady replacement of alcohol by the silyl ether over time induces a significant drop of polarity of greater extent for a 1:1 alcohol:silane starting mixture than for a 2:1 starting mixture. This change in polarity is expected to induce a constant change in ion-pair separation, which may affect the rate of the reaction. In summary, this benchmark clearly points to BArF salts of $[3b]^+$ as the most active in the dehydrosilylation of benzylic alcohol and places them among the possible leading precatalysts for the hydrosilylation of nitriles.

Postulated Mechanism of Autotandem Double Hydrosilylation of Nitriles. Little experimental evidence is known in support of mechanisms at play in the catalytic hydrosilylation of nitriles in general.[10,11b,27] However, most experimental and theoretical studies of hydrosilylation reactions have suggested rather divergent mechanisms, depending on

DOI: 10.1021/acs.organomet.7b00749
Organometallics XXXX, XXX, XXX–XXX

each studied system.[28] In 2010, Nikonov et al. proposed a mechanism of hydrosilylation of nitriles catalyzed by [[Ru](NCMe)(η^2-HSiR$_3$)][B(C$_6$F$_5$)$_4$] intermediates ([Ru] = Ru(^{i}Pr$_3$P)Cp), which supposedly are formed upon reaction of silanes with [[Ru](NCMe)$_2$][B(C$_6$F$_5$)$_4$] precursors.[10] The crucial step was proposed to be the abstraction of the [SiR$_3$]$^+$ moiety from [[Ru](NCMe)(η^2-HSiR$_3$)][B(C$_6$F$_5$)$_4$] by the nitrile substrate to form [[Ru](NCMe)(H)] and a transient silylnitrilium species. This step, invoked in previous DFT-based studies for the carbonyl hydrosilylation reaction, was considered as predominant over the dissociative Ojima-type pathway.[29] More recently, a DFT-supported study conducted by Wu et al. reached similar conclusions.[27a] The authors proposed an outer-sphere silylium abstraction pathway, with the involvement of a "S_N2-Si" transition state as a plausible "*interaction picture*" between the substrates and the Ru catalytic intermediate.

Scheme 3 depicts the proposed idealized mechanism for the catalyzed autotandem double hydrosilylation of nitriles based on our earlier report on the activation of [**3a**]$^+$ leading to silane adduct [**4a**]$^+$.[19b,22] Step 1 is the activation step that converts the solvato−Ir precatalyst into adduct [**4**]$^+$ by consumption of 3 equiv of HSiEt$_3$ per molecule of precatalyst. This crucial step leads to adduct [**4**]$^+$, which holds an Ir-bound silyl group of high electrophilicity, capable of being abstracted by any Lewis base present in the medium. Step 2 corresponds to the abstraction of the SiEt$_3$ "silylium" group, which can be captured by the nitrile substrate in the early stages of the catalysis and by the in situ formed *N*-silylimine intermediate in the later stages of the catalysis to afford *N*-silylnitrilium and *N*-silyliminium cations, respectively.

Scheme 3. Proposed Mechanism of the Autotandem Double Hydrosilylation of Nitriles Catalyzed by Cationic Iridacycles

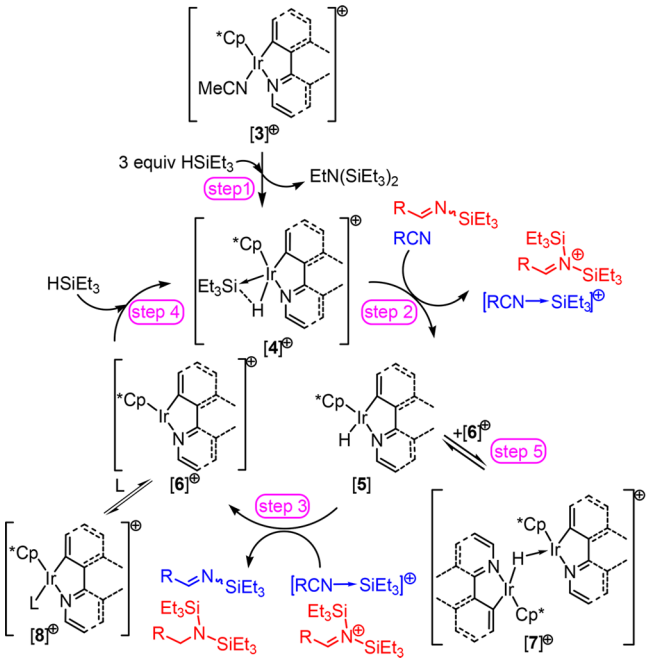

In step 3, the latter cations undergo the transfer of hydride from **5** (**5b**,[30] **5a**[31]) to produce the resulting *N*-silylimine and the *N*,*N*-disilylamine alongside elusive cation [**6**]$^+$. The latter can react either with HSiEt$_3$ (step 4) to regenerate adduct [**4**]$^+$ or, as shown farther (step 5), with **5** to produce the μ-hydrido-bridged bis Ir complex [**7**]$^+$ or with any potential donor ligand present in the medium (nitrile, imine, amine). Under the conditions of the catalysis (T > 298 K, high concentration of RCN substrate, vide infra) this catalytic cycle is a reasonable framework that nonetheless raises a few questions: can the large excess of silane react with highly electrophilic intermediates such as activated nitrile, imine, and the elusive [SiEt$_3$]$^+$ species, as suggested by recent reports published by Oestreich et al.,[32] Chang et al.,[14] and Stephan et al.,[15] and compete with the hydride transfer that is expected to operate from **5**? Do dimeric species [**7**]$^+$ have a role different from that of somewhat sequestrating portions of active Ir species away from relevant catalysis, as reported previously for the *O*-silylation of alcohols?[19b] For convenience, all of the mechanistic investigations deal with in situ characterizations of elementary steps of the catalysis involving either precatalyst [**3b**]$^+$ or [**3a**]$^+$ regardless of the nature of the BArF anion; BArF$_{20}$ is used in place of BArF$_{24}$ in some cases for technical reasons.

Hydrosilylation of Acetonitrile. The starting point was to check whether the hydrosilylation of MeCN with HSiEt$_3$ was possible under catalytic loadings of [**3a**][BArF$_{24}$], using acetonitrile itself as the solvent ("solvent-free" conditions). A blank control experiment consisting of the reaction of MeCN (1 equiv) with HSiEt$_3$ (2 equiv) expectedly resulted in no perceptible conversion (Table 3, entry 1). The same reaction was subsequently conducted in the presence of 1 mol % of [**3a**][BArF$_{24}$] (relative to MeCN) at 50 °C for 44 h (Table 3, entry 2): the monitoring of the reaction mixture by ^{1}H NMR spectroscopy (CD$_2$Cl$_2$, 298 K) revealed the full conversion of MeCN and only a partial conversion of HSiEt$_3$ (∼65%). In addition to the typical signals of the expected product of the double hydrosilylation of MeCN, i.e. N,*N*-bis(triethylsilyl)-ethylamine EtN(Et$_3$Si)$_2$ (characterized by its typical quartet for the Et group at δ 2.86 ppm, J = 7.1 Hz), other signals belonging mainly to two side products were also observed with characteristic peaks of the Et group respectively at δ 3.1 ppm (q, J = 7.1 Hz) and δ 2.76 ppm (qt, J = 7.2 Hz). Electrospray ionization (ESI) mass spectrometry analysis of the reaction mixture confirmed the presence of EtN(SiEt$_3$)$_2$ along with side product **9H$_2$** (vide infra, see spectra in Figures S54 and S55 in the Supporting Information). When the temperature of the reaction medium was raised from 50 to 80 °C, the same mixture of products was noticed even after 100 h of reaction (Table 3, entry 3). Similar features were observed with [**3b**][BArF$_{24}$] as precatalyst under either solvent-free or cosolvent (CH$_2$Cl$_2$) conditions (Table 3, entries 4−7). In addition, the reaction between acetonitrile and other silanes such as HSiPh$_3$ (Table 3, entry 8) and H$_3$SiPh (Table 3, entry 9) under cosolvent conditions (CH$_2$Cl$_2$) proved to give mainly the same mixture of side products in comparison to HSiEt$_3$ (Table 3, entry 7). NMR spectra related to the above results can be found in the Supporting Information.

We decided to further explore the reaction conducted under solvent-free conditions, for which the results are described in entries 2 and 3 of Table 3. ^{1}H NMR spectroscopy analysis indicated that the HSiEt$_3$:MeCN:EtN(Et$_3$Si)$_2$ ratio changed over time from 23:6:1 to 2.2:0:1. This suggests that MeCN was consumed not only by its expected reaction with HSiEt$_3$ to give EtN(Et$_3$Si)$_2$ but also by a secondary reaction with at least one other molecule. It became obvious that at least one of the side products observed throughout the reaction could originate from a coupling reaction between MeCN and another component of the mixture. To solve this issue, the separation

DOI: 10.1021/acs.organomet.7b00749
Organometallics XXXX, XXX, XXX−XXX

Table 3. Investigation of the Hydrosilylation of Acetonitrile and Propionitrile

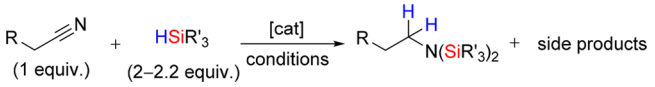

							yield (%)[a] [TON][b]	
entry	R	$HSiR'_3$	[cat.] (amt (mol %))	solvent (0.5 mL)	T (°C)	t (h)	$RCH_2CH_2N(SiR'_3)_2$	side products
1[c]	H	$HSiEt_3$			80	24	<1	<1
2[c]	H	$HSiEt_3$	[**3a**][$BArF_{24}$] (1)		50	44	10 [10]	88
3[c]	H	$HSiEt_3$	[**3a**][$BArF_{24}$] (1)		80	100	14 [14]	86
4[d]	H	$HSiEt_3$	[**3b**][$BArF_{24}$] (1)		80	24	13[13]	53
5[e]	H	$HSiEt_3$	[**3b**][$BArF_{24}$] (0.1)		80	72	2 [20]	13
6[f]	H	$HSiEt_3$	[**3b**][$BArF_{24}$] (0.1)	CH_2Cl_2	60	72	7 [70]	3
7[g]	H	$HSiEt_3$	[**3b**][$BArF_{24}$] (1)	CH_2Cl_2	80	24	8 [8]	10
8[g]	H	$HSiPh_3$	[**3b**][$BArF_{24}$] (1 mol %)	CH_2Cl_2	80	24	<1	78
9[g]	H	H_3SiPh	[**3b**][$BArF_{24}$] (1)	CH_2Cl_2	80	24	2 [2]	2
10[h]	CH_3	$HSiEt_3$	[**3b**][$BArF_{24}$] (1)	CH_2Cl_2	80	24	41 [41]	<1
11[h]	CH_3	$HSiEt_3$	[**3b**][$BArF_{24}$] (1)	CH_2Cl_2	80	72	95 [95]	<1
12[i]	CH_3	$HSiPh_3$	[**3b**][$BArF_{24}$] (1)	CH_2Cl_2	80	24	57 [57]	<1
13[i]	CH_3	H_3SiPh	[**3b**][$BArF_{24}$] (1)	CH_2Cl_2	80	24	2 [2]	<1

[a]Yields are based on the alkylnitrile and were determined by ^{1}H NMR spectroscopy using 1,3,5-tri-*tert*-butylbenzene as internal reference. [b]TON: turnover number, calculated at the highest conversion as the molar ratio of product to initial precatalyst. [c]Conditions: acetonitrile (0.5 mL, 9.7 mmol), $HSiEt_3$ (3.1 mL, 19.4 mmol), [**3a**][$BArF_{24}$] (134.4 mg, 97 μmol), molar ratio nitrile:silane:precatalyst = 100:200:1. [d]Conditions: acetonitrile (0.2 mL, 3.8 mmol), $HSiEt_3$ (1.34 mL, 8.4 mmol), [**3b**][$BArF_{24}$] (53.8 mg, 38 μmol), molar ratio nitrile:silane:precatalyst = 100:221:1. [e]Conditions similar to those in entry 4, except that 5.4 mg of [**3b**][$BArF_{24}$] was used (3.8 μmol), molar ratio nitrile:silane:precatalyst = 1000:2210:1. [f]Conditions: acetonitrile (1 mL, 19.2 mmol), $HSiEt_3$ (6.73 mL, 42.1 mmol), precatalyst (27 mg, 19 μmol), molar ratio nitrile:silane:precatalyst = 1010:2216:1. [g]Conditions: acetonitrile (0.1 mL, 1.9 mmol), $HSiR'_3$ (4.2 mmol), [**3b**][$BArF_{24}$] (27 mg, 19 μmol), molar ratio nitrile:silane:precatalyst = 100:221:1. [h]Conditions: propionitrile (0.2 mL, 2.8 mmol), $HSiEt_3$ (1 mL, 6.2 mmol), [**3b**][$BArF_{24}$] (39.5 mg, 28 μmol), molar ratio nitrile:silane:precatalyst = 100:221:1. [i]Conditions: propionitrile (0.1 mL, 1.4 mmol), $HSiR'_3$ (0.5 mL, 3.1 mmol), [**3b**][$BArF_{24}$] (20 mg, 14 μmol), molar ratio nitrile:silane:precatalyst = 100:221:1.

of the reaction mixture components was attempted. Bulb-to-bulb distillation under vacuum of the latter reaction mixture yielded two main fractions (named respectively fractions 1 and 2). Fraction 1 (obtained at ~70 °C/10 mmHg) contained a coupling product which was structurally identified by ^{1}H and ^{13}C NMR spectroscopy as **9H$_2$**, i.e. the product of the desilylative hydrolysis of the coupling product **9** (Figure 3).

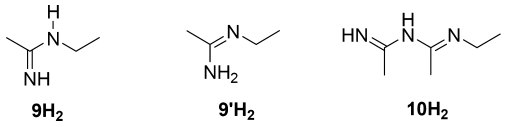

Figure 3. *N*-ethyl-ethanimidamide **9H$_2$**, its tautomer **9′H$_2$**, and **10H$_2$**.

Whereas typical signals for **9** were usually observed in the hydrosilylation reaction mixture at respectively δ(^{1}H, CD_2Cl_2) 3.12 ppm (q, J = 7.1 Hz, $-NCH_2-CH_3$) and 2.01 ppm (s, $-(N{=})C-CH_3$), those of isolated **9H$_2$** resonate at slightly different chemical shifts, i.e. at respectively δ(^{1}H, $CDCl_3$) 3.16 ppm (q, J = 7.0 Hz, $-NCH_2-CH_3$) and 1.94 ppm (s, $-(N{=})C-CH_3$). The molecular structure of **9H$_2$** was further confirmed by X-ray diffraction analysis of single crystals grown by slow evaporation of a pure sample of fraction 1 at −30 °C for around 3 months. Due to the instability of the latter crystals, their elemental analysis afforded three inconsistent values, the first one being the closest to the expected theoretical value (see the Experimental Section for characterization data as well as the related NMR spectra depicted in the Supporting Information). The crystal lattice was found to consist of compound **9H$_2$** and its tautomer **9′H$_2$** (Figure 3). The molecular structure of both compounds is depicted in Figure 4 (vide infra and the

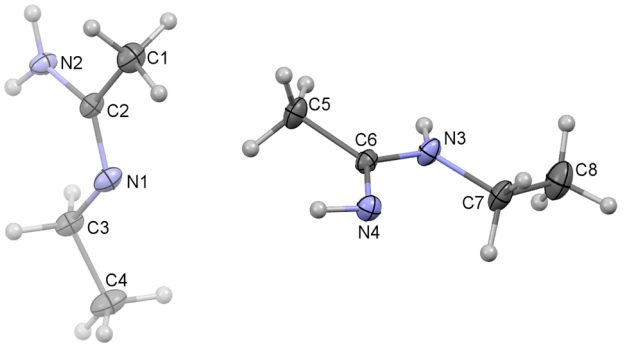

Figure 4. ORTEP-type diagrams of **9H$_2$** (right) and **9′H$_2$** (left) in the asymmetric unit drawn at 30% probability. Selected interatomic lengths (Å) and angles (deg): C1−C2 1.5103(19), C2−N1 1.2872(18), C2−N2 1.3540(16), C3−N1 1.4644(18), C3−C4 1.515(2), C5−C6 1.5142(19), C6−N4 1.3014(18), C6−N3 1.3394(18), C7−N3 1.4518(18), C7−C8 1.492(3), C2−N1−C3 117.15(11), C6−N3−C7 121.55(12).

Supporting Information for further details). ESI mass spectrometry analysis of fraction 1 indicated the presence of **9H** as the major product: i.e., the product of the desilylative hydrolysis of one N−Si bond in **9** (m/z [**9H** + H]$^+$ = 201.2 Da, cf. Figure S56 in the Supporting Information). The second fraction (obtained at ~100 °C; 10 mmHg) contained a 1.3:1 mixture of mainly the two desilylated coupling products **9H$_2$** and **10H$_2$**, respectively (Figure 3). Compound **10H$_2$** was identified by ^{1}H and ^{13}C NMR spectroscopy (cf. Figures S50−S52 in the Supporting Information) as the coupling product of **9′H$_2$** with acetonitrile. Single crystals were grown by slow evaporation of pure sample of fraction 2 at −30 °C for around 3 months. X-ray diffraction analysis of the latter single crystals

DOI: 10.1021/acs.organomet.7b00749
Organometallics XXXX, XXX, XXX−XXX

revealed structures identical with those obtained from fraction 1: i.e., $\mathbf{9H_2}$ and $\mathbf{9'H_2}$. One portion of the reaction mixture which was not submitted to the procedure of distillation was kept for ca. 1 month at −30 °C, after which a precipitate was collected. ^{1}H spectroscopy analysis of the latter solid indicated a spectroscopic signature similar to that of $\mathbf{9H_2}$ (cf. Figure S53 in the Supporting Information).

Crystals of each fraction were submitted to X-ray diffraction analysis. A crystal of the first fraction was found to belong to space group *C*2*c* with three independent molecules within the asymmetric unit: that is, *N*-ethylethanimidamide $\mathbf{9H_2}$ and its tautomer $\mathbf{9'H_2}$ in a 2:1 ratio (Figure 3). The crystal of the second fraction that matched space group $P2_1/c$ contained $\mathbf{9H_2}$ and $\mathbf{9'H_2}$ in a 1:1 ratio. Figure 4 displays the content of the asymmetric unit of the latter crystal.

We postulate that **9** results from the coupling reaction of MeCN with the product of double hydrosilylation of MeCN: i.e., $EtN(Et_3Si)_2$ (Scheme 4). The latter process might be promoted by salts [**3a**,**b**][$BArF_{24}$], which may activate MeCN by coordination toward the nucleophilic attack by $EtN(SiEt_3)_2$. However, at this stage one cannot exclude alternative mechanisms, which would involve as coupling partners either free or coordinated MeCN and ethylamine: i.e., the desilylated form of $NEt(SiEt_3)_2$. Nikonov et al. reported similar observations in 2010.[10] When acetonitrile and $HSiPhMe_2$ were subjected to 0.4 mol % of [$CpRu(PiPr_3)(MeCN)(HSiR_3)$][$B(C_6F_5)_4$] (Scheme 1b) under solvent-free conditions (23 h, ambient temperature), the authors noticed that 95% of MeCN was converted into the desired product $CH_3(H)C{=}NSiPhMe_2$ (10%) and a coupling product identified to be $CH_3(H)C{=}NCH(CH_3)N(SiMe_2Ph)_2$ (60%) and other unknown products. The authors proposed that $CH_3(H)C{=}NCH(CH_3)N(SiMe_2Ph)_2$ might result from the "*N*−*Si addition across the C*═*N bond*". Unfortunately, no further evidence was provided.

Scheme 4. Proposed Mechanism for the Formation of 9

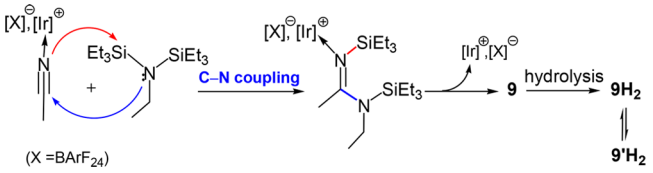

Methods for the catalytic coupling reactions of amines with nitriles are well established.[33] For example, Bochkarev et al.[33a] described the amination of acetonitrile by various amines, such as *i*-$PrNH_2$ and *n*-$PrNH_2$, which was found to be promoted by lanthanide iodides LnI_2 (Ln = Pr, Nd, Dy, Tm). Interestingly, the X-ray structure obtained by the authors for the coupling product of MeCN with ^{i}$PrNH_2$, i.e. $MeC(=NH)NH^iPr$, is very similar to the structure obtained for $\mathbf{9H_2}$ (and its tautomer $\mathbf{9'H_2}$).

In addition, the protons of the Me group (i.e. $MeC(=NH)NH^iPr$) resonate at δ 1.94 ppm (s) in the ^{1}H NMR spectrum ($CDCl_3$, 200 MHz). This is consistent with the data obtained for $\mathbf{9H_2}$, for which a chemical shift at δ 1.94 ppm (s) was observed for the Me protons ($CDCl_3$, 500 MHz) (see full NMR data provided in the Experimental Section). In the course of the present study, it was found that d_6-$\mathbf{9H_2}$ can also be formed by hydrosilylation of CD_3CN with $HSiEt_3$ at room temperature and even at very low temperature (−50 °C) (CD_2Cl_2, [**3a**][$BArF_{24}$] (10 mol % relative to CD_3CN)) (vide infra).

Hydrosilylation of Propionitrile (EtCN). Upon heating at 80 °C for 24 h a reaction mixture containing EtCN (1 equiv), $HSiEt_3$ (2.2 equiv), and [**3b**][$BArF_{24}$] (1 mol % relative to EtCN), the desired product 1,1,1-triethyl-*N*-propyl-*N*-(triethylsilyl)silanamine, i.e. $PrN(SiEt_3)_2$, was formed in 41% yield (Table 3, entry 10). However, when the heating was

Table 4. Investigation of the Hydrosilylation of Benzonitrile by Various Silanes

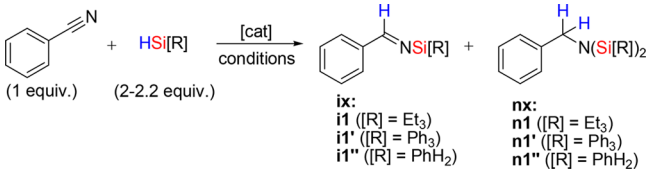

entry	HSi[R]	[cat.] (amt (mol %))	solvent (0.5 mL)	*t* (h)	yield[a] (%) [TON][b] **ix**	**nx**
1[c]	$HSiEt_3$	[**3a**][$BArF_{24}$] (1)		20	>99 [100]	<1
2[d]	$HSiEt_3$	[**3a**][$BArF_{24}$] (1)		24	<1	>99 [100]
3[e]	$HSiEt_3$	[**3b**][$BArF_{24}$] (0.001)	CH_2Cl_2	72	<1	<1
4[f]	$HSiEt_3$	[**3b**][$BArF_{24}$] (1)	CH_2Cl_2	0.1	>99 [100]	<1
5[f]	$HSiEt_3$	[**3b**][$BArF_{24}$] (1)	CH_2Cl_2	48	30 [30]	70 [70]
6[g]	$HSiEt_3$	[**3b**][$BArF_{24}$] (1)	CH_2Cl_2	24	<1	>99 [100]
7[g]	$HSiPh_3$	[**3b**][$BArF_{24}$] (1)	CH_2Cl_2	24	42 [42]	11 [11]
8[g]	H_3SiPh	[**3b**][$BArF_{24}$] (1)	CH_2Cl_2	24	<1	<1

[a]Yields are based on PhCN and were determined by ^{1}H NMR spectroscopy using 1,3,5-tri-*tert*-butylbenzene as internal reference. [b]TON: turnover number, calculated at the highest conversion as the molar ratio of product to initial precatalyst. [c]Conditions: benzonitrile (1 mL, 9.7 mmol), $HSiEt_3$ (3.1 mL, 19.4 mmol), [**3a**][$BArF_{24}$] (134.4 mg, 97 μmol), 50 °C, molar ratio nitrile:silane:precatalyst = 100:200:1. [d]Reaction conducted under similar conditions and in the same vessel in comparison to entry 1, except that the temperature was raised from 50 to 80 °C. [e]Conditions: benzonitrile (1 mL, 9.7 mmol), $HSiEt_3$ (3.4 mL, 19.4 mmol), [**3b**][$BArF_{24}$] (0.5 mL from a 2×10^{-4} M solution in CH_2Cl_2), 70 °C, molar ratio nitrile:silane:precatalyst = 100:200:1. [f]Conditions: benzonitrile (0.18 mL, 1.77 mmol), $HSiEt_3$ (0.62 mL, 3.9 mmol), [**3b**][$BArF_{24}$] (25 mg, 17.7 μmol), 40 °C, molar ratio nitrile:silane:precatalyst = 100:220:1. [g]Conditions: benzonitrile (0.2 mL, 1.94 mmol), HSi[R] (4.23 mmol), [**3b**][$BArF_{24}$] (27.3 mg, 19.4 μmol), 80 °C, molar ratio nitrile:silane:precatalyst = 100:218:1.

DOI: 10.1021/acs.organomet.7b00749
Organometallics XXXX, XXX, XXX−XXX

continued at 80 °C for an additional 48 h (72 h in total), the NMR-based yield in $PrN(SiEt_3)_2$ was ~95% (Table 3, entry 11). Even though $PrN(SiEt_3)_2$, was not isolated, its identity was assessed by its characteristic ^1H NMR spectrum, which is available in Figures S65 and S66 in the Supporting Information. It is worth noting that only the desired product was formed in the case of propionitrile, with the exclusion of any coupling side product. One plausible explanation is that the ethyl group of propionitrile, being a more sterically demanding group than the methyl group of MeCN, makes the formation of side products less favorable. Finally, in comparison to $HSiEt_3$ (Table 3, entry 11), other silanes such as $HSiPh_3$ (Table 3, entry 12) and H_3SiPh (Table 3, entry 13) gave the expected products of autotandem double hydrosilylation of propionitrile in respectively ~57% yield for $HSiPh_3$ and ~2% yield for H_3SiPh.

Hydrosilylation of Benzonitrile. As shown in entries 1 and 2 of Table 4, benzonitrile reacted more readily and selectively with $HSiEt_3$ in comparison to MeCN under the same solvent-free catalytic conditions (Table 3, entry 2). In fact, when the hydrosilylation of 1 equiv of benzonitrile with 2 equiv of $HSiEt_3$ was conducted in the presence of 1 mol % of [**3a**][$BArF_{24}$] (relative to benzonitrile) upon heating at 50 °C for 20 h, ^1H NMR spectroscopic analysis (CD_2Cl_2, 298 K) of the reaction mixture showed the quantitative conversion of benzonitrile (>99%) and the exclusive formation of the product of monohydrosilylation of benzonitrile: i.e., *N*-(triethylsilyl)-benzylimine (**i1**). The identity of **i1** was assessed by ^1H NMR spectroscopy, which showed the presence of a singlet peak at δ 9.06 ppm belonging to the proton of the imino group (i.e., $Ph(C{=}H)N(SiEt_3)$) (our NMR data matched those already reported by Stephan et al.[15]). When the temperature of the reaction mixture was raised from 50 to 80 °C, analysis of the reaction medium after 24 h by ^1H NMR spectroscopy (CD_2Cl_2, 298 K) showed the complete conversion of benzonitrile and the selective and quantitative formation of the product of double hydrosilylation of benzonitrile: i.e., *N*,*N*-bis-(triethylsilyl)benzylamine, (**n1**) (Table 4, entry 2). Product **n1** is characterized by a singlet peak at δ 4.20 ppm, which is typically the NMR signature of a proton bound to an sp^3 carbon atom positioned α relative to a nitrogen atom (i.e., $Ph(CH_2)N(SiEt_3)_2$) (our NMR data matched those already reported by Stephan et al.[15]). Similar results were obtained under cosolvent conditions (CH_2Cl_2). While no reaction occurred with a 0.001 mol % loading of [**3b**][$BArF_{24}$] (Table 4, entry 3), using 1 mol % of precatalyst allowed the selective and quantitative formation of **i1** upon vigorous stirring and moderate heating of the reaction medium to 40 °C for few minutes (reaction conducted in a sealed J. Young NMR tube) (Table 4, entry 4).

When the same reaction mixture (described in Table 4, entry 4) was left to stand at room temperature for additional 48 h, a mixture of **i1** and **n1** was formed in a respective ratio of ~1:2.5 (Table 4, entry 5). The latter result indicates that the room-temperature hydrosilylation of **i1** into **n1** is kinetically less favorable than the hydrosilylation of benzonitrile into **i1**. As a consequence, it seemed mandatory to heat the reaction mixture to at least 70 °C to reduce the reaction time required for the quantitative and exclusive formation of **n1**. This fact was further confirmed during the optimization study described in the next section. In comparison to $HSiPh_3$ (Table 4, entry 7) and H_3SiPh (Table 4, entry 8), $HSiEt_3$ appeared to be the most reactive silane for the hydrosilylation of benzonitrile, giving selectively the desired product in quantitative yield with a TON of 100 (Table 4, entry 6). Under similar conditions, the hydrosilylation of benzonitrile with $HSiEt_3$ (Table 4, entry 6) turned out to be more efficient than that of propionitrile (Table 3, entry 10). This observation is consistent with the expected electron-withdrawing mesomeric activation of arylnitriles in comparison to alkylnitriles that is expressed by an enhanced reactivity of the former toward hydrides. NMR data and assigned NMR spectra related to the results described above are provided in the Supporting Information.

Optimization of the Precatalyst Load for the Hydrosilylation of Benzonitrile with $HSiEt_3$. The influence of the proportion of precatalyst [**3b**][$BArF_{24}$] on the course of the hydrosilylation of benzonitrile was investigated. We first looked at the influence of the proportion of the precatalyst at room temperature and then raised the temperature to 70 °C. The proportion of precatalyst was varied from 0.05 to 1 mol % relative to the concentration of benzonitrile. The conditions for each catalytic run are described in the Experimental Section. This study is summarized in the 3D plot displayed in Figure 5,

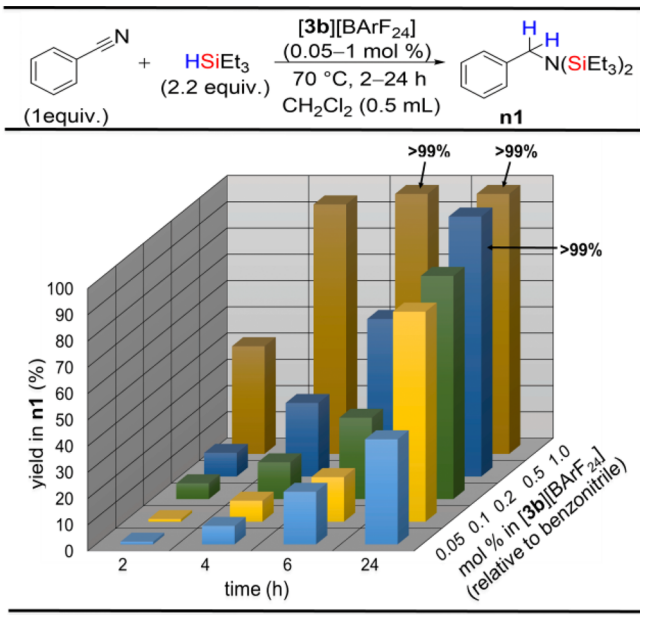

Figure 5. Plot of the yield of **n1** (%) over time (in h) as a function of the loading (mol %) in [**3b**][$BArF_{24}$] in the hydrosilylation of benzonitrile (0.1 mL, 0.97 mmol) by $HSiEt_3$ (0.35 mL, 2.13 mmol) at 70 °C.

which is a plot of the yield (%) of the product of bishydrosilylation of benzonitrile **n1** (*y* axis) vs time (h) (*x* axis) as a function of the proportion (mol %) of [**3b**][$BArF_{24}$] (*z* axis).

It was found that, independently of the initial loading of [**3b**][$BArF_{24}$], no conversion of the substrates occurred at room temperature (see Table S2 in the Supporting Information). However, when the temperature of the reaction mixture was raised to 70 °C, the products of monohydrosilylation (**i1**) and bishydrosilylation (**n1**) of benzonitrile began to appear in the reaction mixture. Through optimization of the proportion of precatalyst [**3b**][$BArF_{24}$] and the time required for quantitative (>99%) and selective formation of the product **n1**, it was found that a loading of 0.5 mol % of precatalyst (relative to benzonitrile) and a reaction time of 24 h constitute optimal conditions for further substrate scope study (vide

DOI: 10.1021/acs.organomet.7b00749
Organometallics XXXX, XXX, XXX–XXX

infra). It is worth noting that using 1 mol % of precatalyst allowed quantitative and selective formation of the product **n1** after only 6 h of reaction at 70 °C (see Table S2 in the Supporting Information for more details). In addition, when only 0.1 mol % of [**3b**][$BArF_{24}$] was used, ^{1}H NMR spectroscopy analysis (C_6D_6, 298 K) after 24 h of reaction showed total conversion of the starting material into **n1** as the major product (~80% yield), along with an unknown compound for which a characteristic singlet peak appeared at δ 3.55 ppm (see the Supporting Information). The identity of the latter compound is tentatively assigned to the amino product derived from the desilylative hydrolysis of N−Si bonds in **n1**.

Isolation and Structural Characterization of Adduct [4b][$BArF_{24}$] (Step 1, Scheme 3). The procedure previously adopted for the in solutio formation of adduct [**4a**][$BArF_{24}$][19b] was applied for the attempted formation of [**4b**][$BArF_{24}$]. A solution of [**3b**][$BArF_{24}$] in CD_2Cl_2 placed in an NMR sample tube equipped with a J. Young valve at −60 °C was treated with 4.4 equiv of $HSiEt_3$. The ^{1}H NMR spectrum revealed the presence of [**4b**]$^+$, [**7b**]$^+$, $EtN(SiEt_3)_2$, and unreacted $HSiEt_3$ in a respective 1:0.1:1.2:1.2 ratio. The hydridic signal of the Ir−H motif of [**4b**]$^+$ was located at −11.4 ppm surrounded by weak satellites assigned to a ^{1}H−^{29}Si coupling constant of 20.0 Hz. The Cp* ligand produced a signal at 1.69 ppm. The Et groups of the $SiEt_3$ moiety appeared at 0.56 ppm as a triplet (Si−CH_2CH_3) and as a set of multiplets of doublets at 0.29 and 0.22 ppm (Si−CH_2CH_3) respectively. ^{29}Si NMR of the same sample produced a signal at 6.92 ppm for the Ir-bound $SiEt_3$ moiety. 2D ^{1}H−^{29}Si HMQC NMR analysis showed a clear cross-correlation peak between signals of the Ir-bound hydride (^{1}H −11.4 ppm) and the $SiEt_3$ group (^{29}Si 6.92 ppm) (cf. Figure S40 in the Supporting Information). Cation [**7b**]$^+$ was firmly identified from its typical hydridic resonance at −22.6 ppm (see the Experimental Section and the Supporting Information). Isolation of a pure sample of [**4b**]$^+$, which was attempted in several instances, was eventually forsaken due to its high reactivity. Crystal growth by diffusion of layered solvents in a narrow sample tube was also a tricky challenge, for solutions of preformed [**4b**][$BArF_{24}$] tended to decompose invariably to give red crystals of [**7b**][$BArF_{24}$] at +4 °C. Crystals of [**4b**][$BArF_{24}$] were successfully obtained by a modification of the crystal growth procedure. Adduct [**4b**][$BArF_{24}$] was synthesized directly in a narrow so-called diffusion glass tube at 4 °C from a solution of [**3b**][$BArF_{24}$] in 1,2-dichloroethane, over which was carefully deposited a small layer of dry and degassed benzene itself topped with a solution of excess $HSiEt_3$ in *n*-hexane. This procedure that used benzene as a solvent diffusion buffer obviously had the advantage of retarding the early formation of [**7b**][$BArF_{24}$] and ensuring the steady growth of crystals of [**4b**][$BArF_{24}$] that were collected for X-ray diffraction analysis.

The resolved structure of the latter salt displayed similarities with that of [**4a**][$BArF_{24}$] (Figure 6a, see also the CIF files and Table S10 in the Supporting Information for acquisition and refinement data).[53] The hydridic hydrogen atom was localized from a difference Fourier map, affording Ir−H and H−Si interatomic distances of ca. 1.49 and 1.60 Å, respectively. The more accurate Ir−Si distance of 2.573(3) Å matches the value already reported for [**4a**][$BArF_{24}$].[19b]

Geometry optimization (cf. the Supporting Information for computational details) at the ZORA-PBE0-dDsC[35] (all-electron triple-ζ single polarized basis set) level provided a gas-phase geometry slightly different from that resolved by X-ray diffraction analysis, displaying expectedly a slightly shorter Si−Ir distance and longer C_{Ar}(C11)−Ir and N−Ir distances (Figure 6b). It is worth noting that the Ir−H (1.58 Å) and Si−H (1.93 Å) interatomic distances are significantly different from those suggested by X-ray diffraction data. This expected discrepancy stems not only from the inaccurate localization

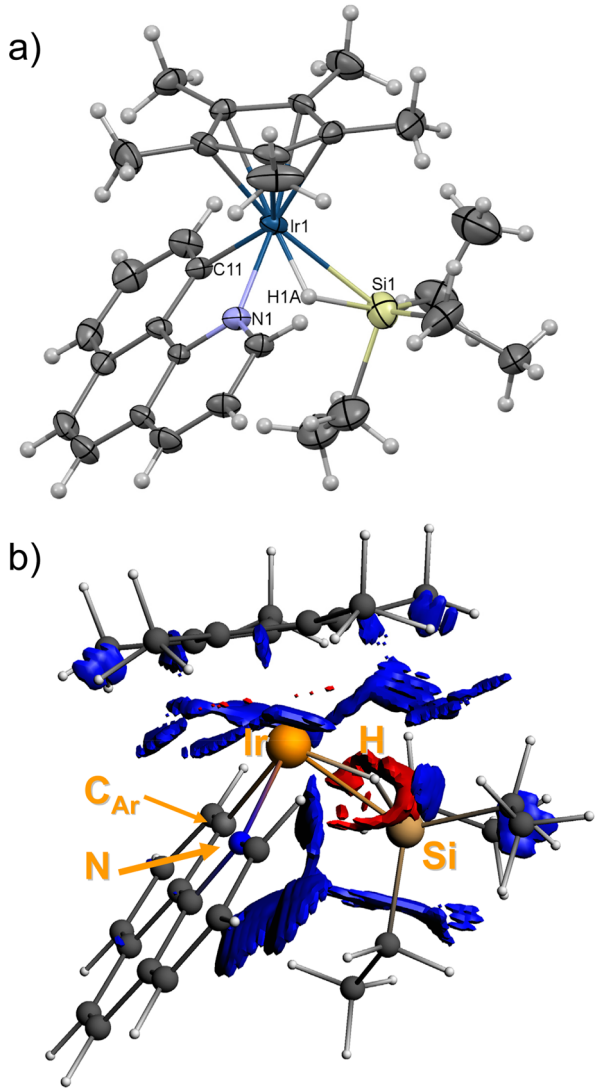

Figure 6. (a) ORTEP-type diagram of cation [**4b**]$^+$ drawn at 30% probability. The SQUEEZE procedure was applied to residual electron density assigned in the lattice to *n*-hexane. For the sake of clarity, the counteranion [$BArF_{24}$]$^-$ and the position-disordered C and H atoms (50% occupation probability) of the $SiEt_3$ moiety are omitted. The position of the hydridic H1A atom was localized from a difference Fourier map and refined. Selected interatomic lengths (Å) and angles (deg): C11−Ir1 2.079(6), N1−Ir1 2.106(5), Si1−Ir1 2.573(3), Ir1−H1A 1.49, Si1−H1A 1.60, Si1−Ir1−H1A 35.0, N1−Ir1−Si1 81.65(17), N1−Ir1−H1A 47.3, C11−Ir1−N1 78.4(2). (b) ADFview[34] plots of noncovalent interaction (NCI) regions materialized by reduced density gradient isosurfaces (cutoff value s = 0.02 au, ρ = 0.05 au) colored according to the sign of the signed density $\lambda_2\rho$ for the gas-phase relaxed singlet ground state model of [**4b**]$^+$: red and blue are associated with negatively (attractive) and positively (repulsive or van der Waals) signed terms, respectively. Selected interatomic lengths (Å) and angles (deg) in the computed model of [**4b**]$^+$: C_{Ar}−Ir 2.120, N−Ir 2.090, Si−Ir 2.503, Ir−H 1.583, Si−H 1.928, Si−Ir−H 39.2, N−Ir−Si 97.0, N−Ir−H 79.3, C_{Ar}−Ir−N 77.2.

DOI: 10.1021/acs.organomet.7b00749
Organometallics XXXX, XXX, XXX−XXX

of the hydridic H atom from the Fourier map but also from the weakness of the Ir−Si interaction that might allow slight structural distortions as a response to strains caused by crystal packing.

The strength of the donor−acceptor (Ir−H)→$[SiEt_3]^+$ interaction[19b,22] in the model of $[\mathbf{4b}]^+$ was evaluated by computing the intrinsic interaction energy ΔE_{int} assuming a fragmentation of the molecule into the neutral "prepared" fragment **5b** and the "prepared" $[SiEt_3]^+$ moiety, the term "prepared" meaning that the original geometry of each fragment was kept as in cation $[\mathbf{4b}]^+$. ΔE_{int} in the latter complex was found to amount to −119 kcal/mol, which is exactly the same value as that found for $[\mathbf{4a}]^+$.[19b,22] Further investigation of the electron density topology using the quantum theory of atoms in molecules[36,37] (QTAIM) revealed that two bond critical points (3,−1) and bond paths exist for Ir−Si and the Ir−H (Figure 7).[19b,22] This situation is akin to

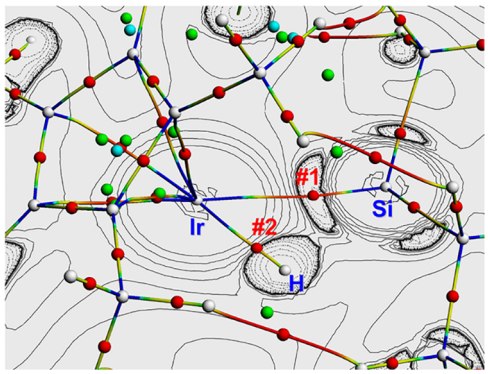

Figure 7. Contour plot of the Laplacian of the density $\nabla^2\rho(r)$[36] for the singlet ground state geometry of $[\mathbf{4b}]^+$ (ZORA-PBE0-dDsC[35]/all electron TZP level, dashed contours correspond to $\nabla^2\rho(r) < 0$) determined in the Ir−Si−H plane and overlaid with a 3D representation of the QTAIM analysis displaying bond critical points (BCP, red dots), ring critical points (green dots), and bond paths (colored by density). BCP (3,−1) #1: ρ = 0.0721 au, $\nabla^2\rho$ = −0.0557 au. BCP(3,−1) #2: ρ = 0.1603 au, $\nabla^2\rho$ = 0.0427 au.

that already reported for $[\mathbf{4a}]^+$, for which it was established that the Si−H interaction was evanescent.[19b] The Wiberg bond indices[38] for the Ir−H (0.47), Ir−Si (0.38), and Si−H (0.23) interactions are consistent with the results of the QTAIM analysis, suggesting a weak Si−H interaction.

Hydride Transfer to the *N*-Silylnitrilium Intermediate (Step 3, Scheme 3). We already established in a previous report that the adduct $[\mathbf{4a}][BArF_{24}]$ was a potential source of electrophilic silyl group[32b,39]—or "silylium"—responsible for the double hydrosilylation of the MeCN ligand in the precatalyst activation step. It is therefore assumed that under catalytic conditions (70 °C, large excess of ArCN) the $[SiEt_3]^+$ moiety of either $[\mathbf{4a}]^+$ or $[\mathbf{4b}]^+$ could readily be captured by the arylnitrile substrate to generate a transient electrophilic *N*-silylnitrilium. In this set of experiments, the formation of the putative *N*-silylnitrilium was attempted to verify the pertinence of step 3 (Scheme 3) that entails the transfer of hydride from **5b**[30,40] to the nitrilium and the formation of a *N*-silylimine. Such an organic cation, i.e. $[RCN\text{-}SiEt_3]^+$, can be considered as a solvated form of the silylium cation. According to the literature,[41] $[SiR_3]^+$ cations can bind up to two nitrile donor ligands, giving rise to the pentacoordinate Si species $[RCN{-}Si(R_3){-}NCR]^+$.[42]

We first attempted to produce this cation by the reaction of TfO−$SiEt_3$ with MeCN in CD_2Cl_2. Careful scrutiny of the ^{1}H NMR spectrum of the resulting solution did not reveal the characteristic signal of the Si-bound acetonitrile.[42b] Further addition of **5b** to this solution did not produce any of the products expected for the reduction of MeCN. Alternatively, we opted for a more drastic procedure entailing the production of a strongly electrophilic $[SiEt_3]^+$ moiety by the abstraction of the hydride from $HSiEt_3$ using the $BArF_{20}$ tritylium salt: i.e., $[Ph_3C][BArF_{20}]$ (Scheme 5).[32a,43] In a first experiment, 1 equiv

Scheme 5. Electrophilic Activation of MeCN by $[SiEt_3]^+$ Followed by Hydride Transfer from 5b

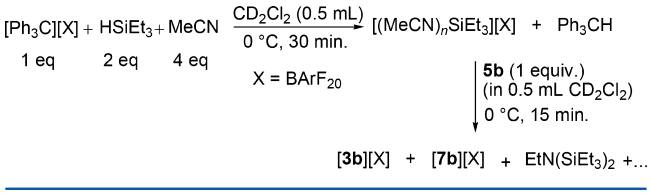

of the latter salt was mixed with ca. 4 equiv of MeCN dissolved in dry CD_2Cl_2 at 0 °C. The mixture was placed in an NMR sample tube equipped with a J. Young valve, and ca. 2 equiv of $HSiEt_3$ was added. The ^{1}H NMR spectrum measured immediately after homogenization of the solution revealed the quantitative formation of Ph_3CH, the presence of unreacted $HSiEt_3$ and a minor amount of *O*-silylated isopropyl alcohol in a 1:0.6:0.5 ratio, the latter probably originating from a contamination of the NMR sample tube by acetone. It was indeed shown by Oestreich et al.[32a] that the tritylium/silane combination could efficiently promote the catalytic reduction of imines. Forcefully, we assume that the O-silated isopropyl alcohol results from such a catalyzed reaction. Nonetheless, the presence of a new species formulated as $[(MeCN)_nSiEt_3]^+$ ($n \geq 1$) could not be firmly established, for its expected signals in ^{29}Si and ^{1}H NMR were not detected. However, a group of signals at δ 2.13 (broad singlet, CH_3), 0.93 (*t*, 9H, $CH_3{-}CH_2Si$), and 0.52 (*q*, 6H, $CH_3{-}CH_2Si$) ppm were assigned to the methyl group of protonated acetonitrile and to the ethyl groups of the $SiEt_3$ moiety of a disiloxane that was already reported in another study by Oro et al.[44] To support this assertion, ^{29}Si NMR of the same solution gave a new singlet at 8.92 ppm that can readily be assigned to $O(SiEt_3)_2$.[44] It is worth noting that a broad peak attributed to a solvated proton was also observed at 11.6 ppm[45] (Figure S73 in the Supporting Information), along with a singlet peak assigned to dissolved H_2 at ca. 4.6 ppm (Figure S74 in the Supporting Information). The origin of the latter signals and of the disiloxane can be explained by the presence of residual water contamination in either of the used reagents or solvent. This solution was subsequently treated at 0 °C with a solution of **5b** in CD_2Cl_2, and the sealed NMR tube was submitted to NMR analyses. The latter clearly revealed the quantitative consumption of **5b** and its conversion into $[\mathbf{3b}][BArF_{24}]$ and $[\mathbf{7b}][BArF_{24}]$ in a 1:1.9 ratio. Furthermore, the typical signals at δ 3.65, 2.83, and 2.75 ppm indicated the formation of $EtN(SiEt_3)_2$ and coupling derivatives (cf. the Experimental Section and Supporting Information). No signals pertaining to the *N*-silyl imine $MeCH{=}NSiEt_3$ were perceptible at this stage of the experiment, suggesting that the second hydrosilylation step implying the formal reduction of the *N*-silyliminium $[MeCH{=}N(SiEt_3)_2]^+$ was much too fast to allow detection of the imine. It is worth noting that the

DOI: 10.1021/acs.organomet.7b00749
Organometallics XXXX, XXX, XXX−XXX

presence of unreacted $HSiEt_3$ left after the reaction with $[Ph_3C][BArF_{20}]$ and moreover the absence of any trace of $EtN(SiEt_3)_2$ before the addition of **5b** suggest that the silane is not a source of hydride of sufficient reactivity to compete with **5b** in the first hydrosilylation of the nitrile function.

The formation of the $[(MeCN)_nSiEt_3]^+$ adduct was attempted de novo by using a $[Ph_3C][BArF_{20}]$:$HSiEt_3$ ratio of 1:0.7 at 0 °C in CD_2Cl_2. In this new experiment, ^1H NMR analysis of the resulting solution at −30 °C revealed a first group of signals at 0.82 (q, J = 8 Hz), 0.98 (t, J = 8 Hz) ppm and at δ 1.05 (m) ppm in a rough 2:1 ratio that were assigned to two different $[(MeCN)_nSiEt_3]^+$ species (cf. Figure S78 and S79 in the Supporting Information). These signals were correlated by a HMQC experiment with two ^{29}Si NMR signals at δ 45 and 42 ppm (respective ratio ca. 2:1, cf. Figure S81 in the Supporting Information). Edlund, Cremer, et al.[42b] stressed that the chemical shift of ^{29}Si was strongly environment sensitive, displaying a wide span of chemical shifts depending on the number of Si-bound donor molecules and on the solvents used in the NMR experiments.[46] However, the published ^{29}Si chemical shifts for triethylsilylnitrilium salts in various solvents are often reported above δ +30 ppm.[42b,46] The associated methyl ^1H NMR signal of the Si-bound MeCN molecule was located at δ 2.30 ppm.[46b] Again at around δ +11.4 ppm the ^1H NMR spectrum suggested the presence of some solvated proton species (solvated proton:$[(MeCN)_nSiEt_3]^+ \approx$ 1:08). To this solution was added a substoichiometric amount of **5b** (relative to $HSiEt_3$) at −30 °C. The ^1H NMR spectrum of the resulting solution revealed the full consumption of **5b**, the formation of $[\mathbf{3b}]^+$, and the absence of any of the signals previously assigned to $[(MeCN)_nSiEt_3]^+$ (cf. Figure S80 in the Supporting Information). New signals at δ 0.48 (m), 0.88 (t), 2.04 (broad s), and 4.8 (s) ppm could not be assigned with certainty. We hypothesize that the latter signals could be related to some form of H_2-based "encounter complex" putatively engaged in an interaction with MeCN and $[SiEt_3]^+$.[47] No acetonitrile hydrosilylation product was detected in this experiment.

Reversible Formation of $[7]^+$ (Step 5, Scheme 3). As mentioned above, crystals of $[\mathbf{7b}][BArF_{24}]$ were obtained from the first failed attempts to grow crystals of $[\mathbf{4b}][BArF_{24}]$. The structure of the cation of the former salt is displayed in Figure 8. This μ-hydrido-bridged bis-iridium complex has the relative R_{Ir}*,R_{Ir}* configuration at each stereogenic Ir center (Figure 8). Although from a crystallographic standpoint no C_2 symmetry axis formally exists, in solution such a symmetry element that bisects perpendicularly the Ir1−Ir2 segment through atom H1A is plausible, as suggested by the ^1H NMR spectrum of $[\mathbf{7b}]^+$ that reveals a single set of aromatic proton signals (cf. the Experimental Section).

Owing to its reactivity and to the lack of stability in the dry solid state, the quest for an analytically pure sample of $[\mathbf{7b}][BArF_{24}]$ was not further pursued. However, several experiments indicate that either $[\mathbf{7a}]^+$ or $[\mathbf{7b}]^+$ should be better considered here as a resting state of the autotandem double hydrosilylation reaction (Scheme 6 and Figures S82−S88 in the Supporting Information). It was found that the reaction of a slight excess of $[\mathbf{3a}][BArF_{24}]$ (2.5 equiv) with **5a** at room temperature in CD_2Cl_2 (J. Young NMR sample tube) produced quantitatively $[\mathbf{7a}][BArF_{24}]$ and free acetonitrile in a 1:1 ratio. Addition of a large excess of MeCN (ca. 50 equiv) converted ca. 50% of $[\mathbf{7a}][BArF_{24}]$ back into **5a** (Scheme 6). Similar results were obtained for the reaction of $[\mathbf{3b}][BArF_{24}]$ with **5b** (Scheme 6). To model closely the intervention of the coordinatively unsaturated cation $[\mathbf{6}]^+$ in the formation $[7]^+$, a solution of **5a** was separately treated with 0.5 equiv of $[Ph_3C][BArF_{20}]$ used as a hydride abstraction agent capable of releasing in situ the elusive $[\mathbf{6a}]^+$ intermediate (eq 3). The experiment carried out in a sealed NMR tube at 20 °C in d_5-PhCl indicated the quantitative conversion of **5a** into $[\mathbf{7a}]^+$ (Figure S89 in the Supporting Information).

Low-Temperature Hydrosilylation of MeCN. The reversibility of the formation of the μ-hydrido dimer $[7]^+$ was further confirmed by carrying out the treatment of CD_3CN (10

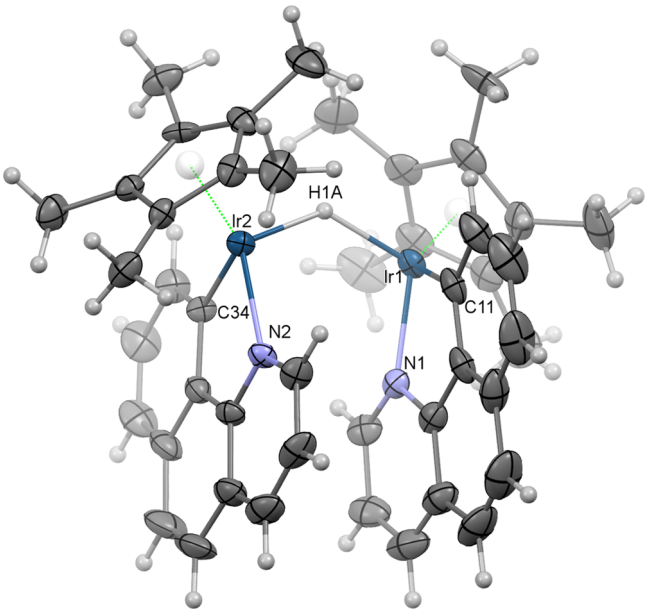

Figure 8. ORTEP-type diagram of cation $[\mathbf{7b}]^+$ drawn at 30% probability. For the sake of clarity, the counteranion $[BArF_{24}]^-$ was omitted. The hydridic H1A atom was localized from a difference Fourier map and refined. Selected interatomic lengths (Å) and angles (deg): C11−Ir1 2.078(4), N1−Ir1 2.088(7), Ir1−H1A 1.86, Ir2−H1A 1.79, C34−Ir2 2.040(7), N2−Ir2 2.090(7), Ir2−H−Ir1, 131.5(1). Cp*−Ir bonding is shown, for the sake of clarity, as a green bond between the white spheres in the center of each cyclopentadienyl ring and the Ir centers.

Scheme 6. Reactivity of 5a,b with Acetonitrile Salts $[\mathbf{3a,b}][X]$[a]

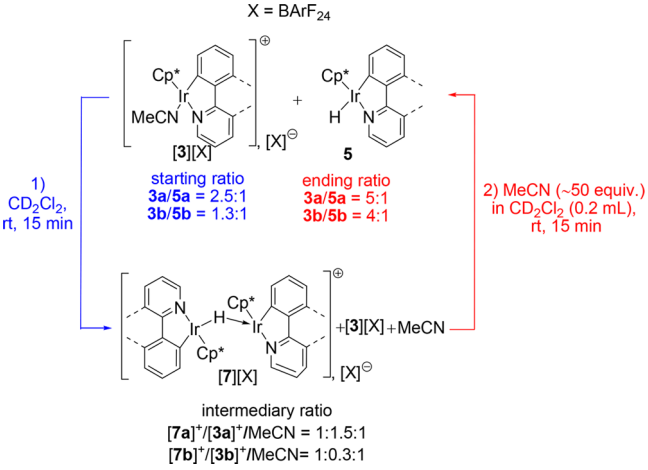

[a]Ratios determined by ^1H NMR.

DOI: 10.1021/acs.organomet.7b00749
Organometallics XXXX, XXX, XXX−XXX

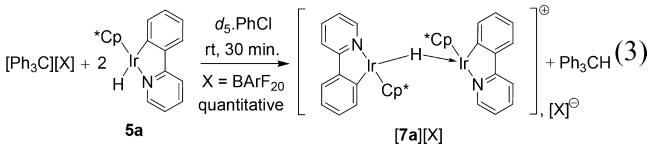

(3)

equiv) with $HSiEt_3$ (20 equiv) in the presence of nearly catalytic amounts of $[\mathbf{3a}][BArF_{24}]$ (1 equiv) in CD_2Cl_2 at −50 °C in a J. Young NMR sample tube. The reaction mixture that was left to react for 60 min was subsequently analyzed by ^1H NMR, revealing the formation of large amounts of $CD_3CH_2N(SiEt_3)_2$ in addition to trace amounts of other organic compounds such as protio and deuterio MeCN ($CD_3CH_2N(SiEt_3)_2$:MeCN ≈ 82:1). Among the organometallic species, one could identify $[\mathbf{7a}]^+$ and the new iridacyclic complex $[\mathbf{8a}]^+$ (Scheme 3, with L = CD_3CN) present in a 1:1.7 ratio on the basis of the integration of their respective Cp* methyl signals. Minor amounts of **5a** were also perceptible. The same experiment carried out at room temperature for 30 min resulted in the complete conversion of CD_3CN into $CD_3CH_2N(SiEt_3)_2$ and trace amounts of a mixture of organic side products displaying ^2H NMR signals at 2.09 and 1.09 ppm. Compound **5a** was the only organometallic species identified in the medium by ^1H NMR spectroscopy.

Hydrosilylation of Benzonitrile and Acetophenone. BArF salts of $[\mathbf{3a–c}]^+$ were further evaluated for the hydrosilylation of acetophenone and benzonitrile, for which reaction conditions were optimized. In all cases the hydrosilylation of acetophenone was completed within 30 min at room temperature using $HSiEt_3$. In turn, the exhaustive hydrosilylation of benzonitrile required an optimal temperature of 70 °C to produce almost quantitatively in 24 h the corresponding *N,N*-bis(triethylsilyl)benzylamine. The amount of precatalyst in all cases was lower than 1 mol % relative to acetophenone and benzonitrile. Tables 5 and 6 give the

Table 5. Hydrosilylation of Benzonitrile at 70 °C

entry	precatalyst	yield[a] (%)	TON[b] (%)
1	$[\mathbf{3a}][BArF_{20}]$	93	188
2	$[\mathbf{3b}][BArF_{20}]$	>99	200
3	$[\mathbf{3a}][BArF_{24}]$	>99	200
4	$[\mathbf{3b}][BArF_{24}]$	>99	200
5	$[\mathbf{3c}][BArF_{24}]$	>99	200

[a]Conditions: benzonitrile (0.10 mL, 0.97 mmol), Et_3SiH (0.35 mL, 2.2 mmol), precatalyst (4.8 μmol, ∼0.5 mol % relative to benzonitrile), CH_2Cl_2 (0.5 mL), 70 °C, molar ratio nitrile:silane:precatalyst = 202:458:1, 24 h. [b]TON: turnover number, calculated at the highest conversion as the molar ratio of product to catalyst.

respective TONs for each type of reaction. The values for the hydrosilylation of acetophenone are roughly 4.5 times greater than those of the double hydrosilylation of benzonitrile for nearly total conversions of the substrates into the respective silyl ether and *N,N*-disilylamine. Quite interestingly all BArF salts promoted the double hydrosilylation of benzonitrile equally at 70 °C, producing TONs of ca. 200 when a 1:2 benzonitrile:silane ratio was used. It is worth noting, however, that other salts, such as $[\mathbf{3b}][OTf]$ and $[\mathbf{3b}][BPh_4]$, did not perform well at all in the hydrosilylation of benzonitrile (Table 7, entries 2 and 3). Experiments run under identical conditions did not yield more than 5% of the double-hydrosilylation product, the starting material being recovered mostly

Table 6. Hydrosilylation of Acetophenone at Room Temperature

entry	precatalyst	yield[a] (%)	TON[b] (%)
1	$[\mathbf{3a}][BArF_{20}]$	>99	970
2	$[\mathbf{3b}][BArF_{20}]$	>99	970
3	$[\mathbf{3a}][BArF_{24}]$	>99	970
4	$[\mathbf{3b}][BArF_{24}]$	>99	970
5	$[\mathbf{3c}][BArF_{24}]$	>99	970

[a]Conditions: acetophenone (0.10 mL, 0.86 mmol), $HSiEt_3$ (0.15 mL, 0.94 mmol), precatalyst (8.6 μmol, 0.1 mol %), CH_2Cl_2 (0.5 mL), room temperature, ratio acetophenone:silane:precatalyst = 1000:1000:1, 30 min. [b]TON: turnover number, calculated at the highest conversion as the molar ratio of product to catalyst.

Table 7. Effect of the Nature of the Counteranion of $[\mathbf{3b}]^+$ on the Double Hydrosilylation of Benzonitrile with $HSiEt_3$

entry	precatalyst	yield (%)[a]
1	$[\mathbf{3b}][BArF_{24}]$	>99
2	$[\mathbf{3b}][OTf]$	5
3	$[\mathbf{3b}][BPh_4]$	1

[a]All reactions were conducted at 70 °C: benzonitrile (0.1 mL, 0.97 mmol), $HSiEt_3$ (0.35 mL, 2.1 mmol), precatalyst (9.7 μmol, 1 mol %), CH_2Cl_2 (0.5 mL).

untouched. The low performance of $[\mathbf{3b}][OTf]$ is putatively assigned to the formation of Et_3SiOTf, which might not display a sufficient electrophilicity toward PhCN to produce efficiently the putative $[Et_3Si(PhCN)_n]^+$ key intermediate. It is hypothesized that a lack of stability in solution might explain the low performance of $[\mathbf{3b}][BPh_4]$ (vide supra).

Hydrosilylation of Nitriles Catalyzed by $[\mathbf{3b}][BArF_{24}]$: Scope. The scope of the catalysis of the double hydrosilylation of nitriles was explored using exclusively arylnitriles containing either electron-withdrawing or -donating substituents as well as potential donor ligands susceptible of challenging the catalysis by catalyst poisoning (Scheme 7, products **n1**–**n14**). Scheme 7 displays the targets that were pursued under the standardized conditions defined for benzonitrile: i.e., 70 °C and 0.5 mol % of catalyst relative to the starting arylnitrile. Almost all nitrile substrates were converted into the corresponding *N,N*-disilylamines in yields spanning 86–99% (**n1**–**n5**, **n7**–**n11**, **n13**, and **n14**) without the formation of any side product. For instance the arylnitrile substrate related to **n6**, i.e. 4-aminobenzonitrile, was left untouched with no *N*-silylation of the amino group or any sign of monohydrosilylation of the nitrile being detected in the ^1H NMR spectrum of the crude reaction mixture. It is speculated that 4-aminobenzonitrile inhibits the catalysis by binding the only coordination site available at the Ir center of $[\mathbf{3b}]^+$ for the activation of the silane.

Such catalyst poisoning is most certainly responsible also for the lack of conversion of 3-cyanopyridine into **n12**, the pyridyl moiety diverting greater amounts of Ir complex into a catalytically inert form. It is interesting to note that 4-hydroxybenzonitrile was efficiently converted into **n11** in a process involving the joint dehydro *O*-silylation of the phenolic hydroxyl substituent and the double hydrosilylation of the nitrile function. Similarly 4-acetylbenzonitrile was nonselectively converted into **n13** by the joint hydrosilylation of the carbonyl and nitrile functions. However, side dehydrogenation occurring at the ketyl function was also observed under certain conditions (Figure S125 in the Supporting Information). It is worth noting that **n14**, a potential precursor of a pincer ligand,

DOI: 10.1021/acs.organomet.7b00749
Organometallics XXXX, XXX, XXX–XXX

Scheme 7. Autotandem Double Hydrosilylation of Arylnitriles: Scope[a]

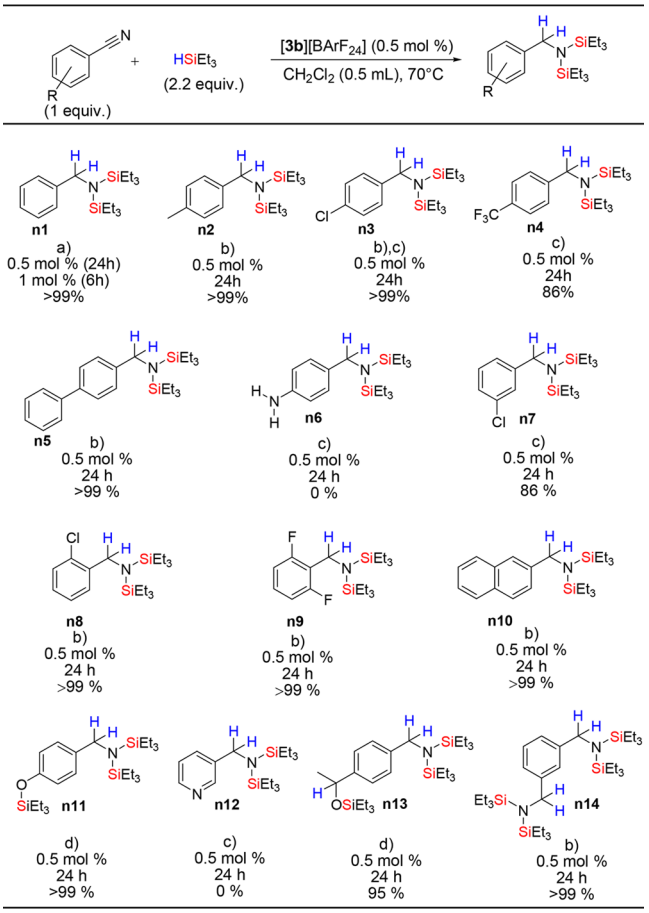

[a]Conditions: (a) nitrile (1.1 mmol), $HSiEt_3$ (0.35 mL, 2.1 mmol), [**3b**][$BArF_{24}$] (6.8 mg, 4.8 mmol [0.5 mol %] or 13.7 mg, 9.7 mmol [1 mol %]), 70 °C; (b) arylnitrile (0.8 mmol), $HSiEt_3$ (0.3 mL, 1.8 mmol), [**3b**][$BArF_{24}$] ([0.5 mol %] or [1 mol %]), 70 °C; (c) conditions similar to those in (b), except that instead of 2.2 equiv of $HSiEt_3$, 4.4 equiv (0.60 mL, 3.7 mmol) was used; (d) conditions similar to those in (b), except that instead of 2.2 equiv of $HSiEt_3$, 8.8 equiv (1.20 mL, 7.5 mmol) was used. Yields were determined by ^{1}H NMR spectroscopy using 1,3,5-tri-*tert*-butylbenzene as internal reference.

was also prepared in high yield by the double hydrosilylation of two nitrile groups.

Investigation of Catalyst Response to Competitive Hydrosilylation Conditions. We gauged the catalytic potential of [**3b**][$BArF_{24}$] and its reactivity toward aldehydes, ketones, and nitriles. The latter precatalyst was placed under competitive reaction conditions consisting of equimolar mixtures of different substrates and $HSiEt_3$. These sets of experiments were expected to produce a qualitative preferential order of reactivity. A first experiment consisting of a reaction of a 1:1:1 mixture of benzaldehyde, acetophenone, and $HSiEt_3$ was carried out at room temperature in CH_2Cl_2 in the presence of 0.1 mol % of [**3b**][$BArF_{24}$] (eq 4). The reaction produced predominantly the benzyl silyl ether (61% yield determined by ^{1}H NMR using 1,3,5-tri-*tert*-butylbenzene as internal reference), suggesting a net preference of the catalytic pot for the hydrosilylation of the aldehyde.

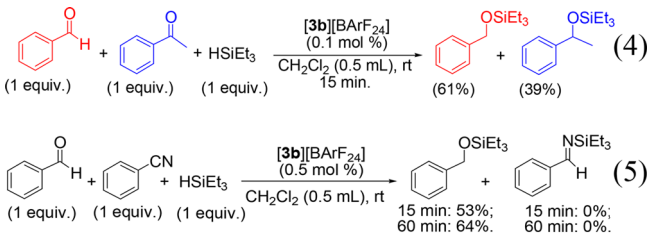

Another experiment was performed with a 1:1:1 mixture of acetophenone, benzonitrile, and $HSiEt_3$ at room temperature with ca. 0.5 mol % of [**3b**][$BArF_{24}$] (eq 5). The reaction, which was monitored by removing aliquots of the reaction medium for ^{1}H NMR spectroscopic investigations at different reaction times, revealed that the hydrosilylation reaction was predominant with benzaldehyde, producing a yield of about 53% after only 15 min. The minor improvement in the yield after 60 min (64% yield) of reaction suggested that benzonitrile might be inhibiting the catalysis and that slightly forcing experimental conditions would be required to achieve its hydrosilylation.

The potential of [**3b**][$BArF_{24}$] in the hydrosilylation of ketones and aldehydes was also investigated on a series of protypical aromatic and aliphatic substrates. The corresponding results are available in Schemes S4 and S5 in the Supporting Information. These results show that the hydrosilylation of carbonyls operates with precatalyst loads of 0.05−2 mol %, producing the resulting triethylsilyl ethers in yields >90% in most cases, this without the use of any additive.[48]

CONCLUSION

Far from being poisoned by nitriles, the cationic Ir(III) metallacycles used in this study perform rather well as catalysts for the autotandem double hydrosilylation of acetonitrile, propionitrile, and a variety of other arylnitriles. In dilute solution, the cationic precatalysts [**3a,b**]$^+$ undergo an energetically unfavorable reaction with $HSiEt_3$, leading to adducts [**4a,b**]$^+$ by a specific concerted hydride transfer reaction and capture of the electrophilic $[SiEt_3]^+$ moiety by the newly formed hydrido-iridium species: the released MeCN molecules are converted into the *N,N*-disilylated ethylamine. Under solventless conditions, i.e. where the concentration of nitrile is overwhelming in comparison to that of the Ir catalyst, the binding of $[SiEt_3]^+$ to the Ir is most certainly swiftly quenched by reaction with the nitrile substrate, giving rise to highly electrophilic forms of reactive nitrilium cations that may hence undergo the nucleophilic transfer of hydride from transient intermediate **5a,b**. Whether the transfer of hydrido ligand occurs once the silylnitrilium is released in the solution bulk or in a somewhat concerted manner upon nucleophilic attack of the Ir-bound silyl moiety by MeCN remains unsettled. Experimental evidence of the noninterference of $HSiEt_3$ as a potential competing source of hydride in the reduction of nitriles also outlines the central role of the iridium-hydrido species **5a,b** as the main source of nucleophilic hydride in this catalytic process indeed. However, owing to the experimental difficulties in observing unambiguously the conversion of $[(MeCN)_nSiEt_3]^+$ into the expected products of hydrosilylation, further investigations seem mandatory both experimentally and theoretically. For the sake of conciseness, theoretical support of the mechanism proposed in Scheme 3 in the form of a full Gibbs catalysis energy profile was not included to the present paper and will be disclosed elsewhere. Species [**7b**]$^+$, i.e. the analogue of [**7a**]$^+$, which was considered

DOI: 10.1021/acs.organomet.7b00749
Organometallics XXXX, XXX, XXX−XXX

as a catalytically inactive diversion of valuable iridacycle in the room-temperature dehydro *O*-silylation of alcohols, should be considered as a resting state under the conditions of the present nitriles' double-hydrosilylation catalysis. The main feature of this catalytic system remains the peculiar mode of formation of adducts $[\mathbf{4a,b}]^+$, the consistent formulation of which as a (Ir−H)→$[SiEt_3]^+$ Ir(III) donor−acceptor complex opens upa new perspective for iridacycles in chemical processes where the elusive highly electrophilic $[SiR_3]^+$ moiety is central.[32,39,41a,49] Recent theoretical investigations tend to suggest that similar bonding situations may well exist in Brookhart's POCOP-Ir catalyst as well as in a number of other situations depicted by Nikonov et al. and Oestreich et al. for example.[22] The potential of this class of iridacycles as multifaceted Lewis acids capable of not only efficiently binding conventional donor ligands but also activating Si−H bonds justifies our quest for "multi-competent" catalysts[19a] capable of promoting complex autotandem type chemical transformations. As iridacycles containing the Cp*Ir moiety are rather easy to synthesize and derive into solvato MeCN cations, their inherent chirality at Ir raises the question of their potential in asymmetric catalysis, which motivates current research that will be disclosed in due time.

EXPERIMENTAL SECTION

General Considerations. All experiments were conducted under a dry argon atmosphere using standard Schlenk and glovebox techniques. All glassware was oven-dried prior to use. All solvents were distilled over sodium or CaH_2 under argon before use. Deuterated solvents were dried over sodium or CaH_2, filtered over activated neutral alumina, and stored under argon before use. Ligands **1a−c**, benzyl alcohol, carbonyls, and nitriles were purchased from Sigma-Aldrich, Alfa Aesar, TCI, and Fluka. $IrCl_3$ was purchased from Pressure Chemical Co. Dicalite 4158 was purchased from Carlo Erba Reagents. Ligands **1b,c** were used as received, while ligand **1a** was purified by bulb-to-bulb distillation over a minimal amount of molecular sieves (MS-3 Å) and stored over MS-3 Å in a Schlenk tube under argon. Benzyl alcohol was purified by bulb-to-bulb distillation over a minimal amount of CaH_2 and stored over MS-3 Å under argon. Nitriles were used as received, whereas liquid carbonyls were purified by bulb-to-bulb distillation over a minimal amount of CaH_2 and stored under argon before use. Ligand name abbreviations: Cp*, 1,2,3,4,5-pentamethyl-η^5-cyclopentadienyl; PhPy, 2-(2-pyridyl)-phenyl, B[*h*]Q, benzo[*h*]quinolinyl; DB[*f,h*]Q, dibenzo[*f,h*]quinolinyl. $[Ir(\mu\text{-Cl})ClCp^*]_2$ was synthesized from $IrCl_3$ and 1,2,3,4,5-pentamethylcyclopenta-1,3-diene following the procedure reported in the literature.[25b] Compounds **2a,b** were prepared following the procedure reported in the literature.[24a,50] Compounds **5a,b** were prepared according to the procedure reported by Templeton et al.,[31b] and their NMR data were found to be similar to those already reported by Norton et al.[30] $[\mathbf{3a}][BArF_{24}]$ was prepared following a published procedure.[19b] The so-called trityl salt $[Ph_3C][BArF_{20}]$ was prepared according to the modified procedure (originally reported by Ozerov et al.[51]) described by Heinekey et al.[52] ^1H (300, 400, 500, and 600 MHz), ^{11}B (128 MHz), ^{13}C (75 and 126 MHz), ^{19}F (282 MHz), and ^{29}Si (119 MHz) NMR spectra were measured on Bruker DPX 300 and 400, Avance I 500, and Avance III 600 spectrometers. All chemical shifts (δ) are expressed in parts per million (ppm). For ^1H and ^{13}C NMR, values of δ are reported relative to Me_4Si as an external reference standard and referenced against peaks of solvents (only partially deuterated solvent is visible in ^1H) as secondary reference standards. For other nuclei, the reported values of δ are referenced to external reference standards ($CF_3C_6H_5$ in $CDCl_3$ for ^{19}F, Me_4Si in $CDCl_3$ for ^{29}Si, and $NaBH_4$ in D_2O for ^{11}B). Abbreviations used for NMR data: s, singlet; d, doublet; t, triplet; q, quartet; qt, quintet; sept, septet; m, multiplet; br, broad; *J*, coupling constant; Ar, aromatic. Mass spectra were run on a MicroTOF Bruker Daltonics spectrometer, using a TOF-ESI coupling analysis system. Elemental analyses were performed with Thermo Scientific FLASH 2000 CHNS/O analyzers. Refer to the Supporting Information for computational details and information on structural X-ray diffraction analyses.

Procedure for the Synthesis of [Cp*Ir(DB[*f,h*]Q)Cl] (2c) (Scheme 2). A Schlenk flask was loaded with the ligand **1c** (150 mg, 0.65 mmol), the iridium precursor $[Ir(\mu\text{-Cl})ClCp^*]_2$ (287 mg, 0.36 mmol), and anhydrous NaOAc (160 mg, 1.95 mmol). To this mixture was added ∼15 mL of CH_2Cl_2. After vigorous stirring at 50 °C for 48 h, the reaction mixture was filtered through Dicalite and the filtrate stripped of solvent under reduced pressure. The resulting residue was then washed with *n*-pentane. The product **2c** was recovered as a yellow-orange powder (231 mg, 60% yield). Anal. Calcd for $C_{27}H_{25}ClIrN\cdot 1/10CH_2Cl_2$: C, 54.57; H, 4.25; N, 2.37. Found: C, 54.76; H, 4.43; N, 2.37. ^1H NMR (500 MHz, 298 K, $CDCl_3$): δ 8.97 (d, 1H, J = 5.3 Hz, *H*−C═N DB[*f,h*]Q), 8.78 (d, 1H, J = 8.4 Hz, H_{Ar} DB[*f,h*]Q), 8.64 (d, 1H, J = 8.4 Hz, H_{Ar} DB[*f,h*]Q), 8.54 (d, 1H, J = 8.4 Hz, H_{Ar} DB[*f,h*]Q), 8.16 (d, 1H, J = 8.0 Hz, H_{Ar} DB[*f,h*]Q), 8.05 (d, 1H, J = 7.2 Hz, H_{Ar} DB[*f,h*]Q), 7.72 (t, 1H, J = 7.2 Hz, H_{Ar} DB[*f,h*]Q), 7.62−7.67 (m, 2H, H_{Ar} DB[*f,h*]Q), 7.52 (d, 1H, J = 8.1 Hz, H_{Ar} DB[*f,h*]Q), 7.50 (d, 1H, J = 8.1 Hz, H_{Ar} DB[*f,h*]Q), 1.75 (s, 15H, Cp-*Me*$_5$). ^{13}C NMR (126 MHz, 298 K, $CDCl_3$): δ 161.9 (DB[*f,h*]Q), 158.4 (DB[*f,h*]Q), 149.8 (H−*C*═N, DB[*f,h*]Q), 140.3 (DB[*f,h*]Q), 133.5 (*C*−H, DB[*f,h*]Q), 132.1 (DB[*f,h*]Q), 132.0 (DB[*f,h*]Q), 131.2 (*C*−H, DB[*f,h*]Q), 128.5 (*C*−H, DB[*f,h*]Q), 128.1 (DB[*f,h*]Q), 127.1 (*C*−H, DB[*f,h*]Q), 126.1 (DB[*f,h*]Q), 124.1 (*C*−H, DB[*f,h*]Q), 123.4 (*C*−H, DB[*f,h*]Q), 122.0 (*C*−H, DB[*f,h*]Q), 115.7 (C−H, DB[*f,h*]Q), 88.7 (*Cp*-Me$_5$), 8.9 (Cp-*Me*$_5$). HRMS-ESI: calcd for $C_{27}H_{25}ClIrN$ ($[\mathbf{2c}]^{\bullet+}$) (*m*/*z*) 591.1292, found 591.1320. HRMS-ESI: calcd for $C_{27}H_{25}IrN$ ($[\mathbf{2c} - Cl]^+$) (*m*/*z*) 556.1612, found 556.1638.

General Procedure for the Synthesis of [3a−c][X] (Scheme 2). In a Schlenk flask an equimolar mixture of **2a−c** and [MX] (MX = $K[BArF_{20}]$, $Na[BArF_{24}]$, $Na[BPh_4]$, or Ag[OTf]) was dissolved in acetonitrile (∼7−10 mL). The resulting mixture was vigorously stirred at room temperature for a period not exceeding 4 h, unless otherwise stated. The resulting suspension was filtered through a pad of Dicalite, and the solvent was removed from the filtrate under reduced pressure. The solid was either recrystallized in a mixture of CH_2Cl_2 and *n*-hexane or *n*-pentane or washed with *n*-hexane or *n*-pentane, to afford an analytically pure compound.

*[Cp*Ir(PhPy)(NCMe)][BArF$_{20}$] ([**3a**][BArF$_{20}$]) (Scheme 2).* This compound was prepared following the general procedure described above: **2a** (300 mg, 0.580 mmol), $K[BArF_{20}]$ (138.6 mg, 0.193 mmol), MeCN (7 mL), room temperature, 2 h. The raw material was purified by recrystallization with a mixture of CH_2Cl_2 and *n*-pentane, and the resulting salt was washed with *n*-pentane and dried under reduced pressure. $[\mathbf{3a}][BArF_{20}]$ was recovered as a yellow powder in 90% yield (629 mg). Single crystals were grown by slow diffusion of hexane into a solution of $[\mathbf{3a}][BArF_{20}]$ in 1,2-dichloroethane (−30 °C). Anal. Calcd for $C_{47}H_{26}BF_{20}IrN_2\cdot CH_2Cl_2$: C, 44.81; H, 2.19; N, 2.18. Found: C, 45.04; H, 2.08; N, 2.25. ^1H NMR (500 MHz, 295 K, CD_2Cl_2): δ 8.62 (d, 1H, J = 5.7 Hz, *H*-C═N PhPy), 7.94 (d, 1H, J = 8.0 Hz, H_{Ar} PhPy), 7.88 (td, 1H, J_1 = 7.8 Hz, J_2 = 1.4 Hz, H_{Ar} PhPy), 7.75 (t, 2H, J = 7.9 Hz, H_{Ar} PhPy), 7.29 (td, 1H, J_1 = 7.5 Hz, J_2 = 1.4 Hz, H_{Ar} PhPy), 7.25 (td, 1H, J_1 = 6.6 Hz, J_2 = 1.4 Hz, H_{Ar} PhPy), 7.20 (td, 1H, J = 7.5 Hz, J_2 = 1.2 Hz, H_{Ar} PhPy), 2.27 (s, 3H, Ir-NC*Me*), 1.68 (s, 15H, Cp-*Me*$_5$). ^{13}C NMR (126 MHz, 295 K, CD_2Cl_2): δ 168.0 (PhPy), 156.6 (PhPy), 151.9 (H-C═N, PhPy), 148.5 (*C*-F, d (br), ^1J = 240.0 Hz, 2C of C_6F_5 in $BArF_{20}$), 145.1 (PhPy), 139.7 (*C*−H, PhPy), 137.6 (*C*-F, m, 1C of *p*-C_6F_5 in $BArF_{20}$), 136.0 (*C*−H, PhPy), 135.7 (*C*-F, m, ^1J = 24.0 Hz, 2C of C_6F_5 in $BArF_{20}$), 132.1 (*C*−H, PhPy), 124.9 (*C*−H, PhPy), 124.5 (*C*−H, PhPy), 124.0 (*C*−H, PhPy), 120.3 (*C*−H, PhPy), 118.4 (Ir−NCMe), 91.8 (*Cp*-Me$_5$), 8.9 (Cp-*Me*$_5$), 4.3 (Ir-NC*Me*), [the 1:1:1:1 quartet characterizing the *C*-B bond in C_6F_5 ($BArF_{20}$) escaped detection]. ^{19}F NMR (282 MHz, 298 K, CD_2Cl_2): δ −133.50 (m, 8F, *o*-C_6F_5 in $BArF_{20}$), −164.04 (t, 4F, $^3J_{F-F}$ = 20.7 Hz, *p*-C_6F_5 in $BArF_{20}$), −167.82 (m, 8F, *m*-C_6F_5 in $BArF_{20}$). ^{11}B NMR (128 MHz, 298 K, CD_2Cl_2): δ −16.7 (s). HRMS-ESI: calcd for $C_{21}H_{23}IrN$ ($[\mathbf{3a} - NCMe]^+$) (*m*/*z*) 482.1455, found 482.1495.

DOI: 10.1021/acs.organomet.7b00749
Organometallics XXXX, XXX, XXX−XXX

*[Cp*Ir(B[h]Q)(NCMe)][BArF$_{24}$] ([**3b**][BArF$_{24}$])* (Scheme 2). This compound was prepared following the general procedure described above: **2b** (150 mg, 0.277 mmol), Na[BArF$_{24}$] (245.7 mg, 0.277 mmol), MeCN (7 mL), room temperature, 3 h. After recrystallization with a mixture of CH_2Cl_2 and *n*-pentane the product was washed with *n*-pentane and the resulting yellow powder of [**3b**][BArF$_{24}$] was isolated in 93% yield (363 mg). Single crystals were grown by slow diffusion of a mixture of hexane and benzene into a solution of [**3b**][BArF$_{24}$] in 1,2-dichloroethane. Anal. Calcd for $C_{57}H_{38}BF_{24}IrN_2 \cdot 1/10CH_2Cl_2$: C, 48.35; H, 2.71; N, 1.98. Found: C, 48.56; H, 2.72; N, 1.99. ^{1}H NMR (500 MHz, 298 K, CD_2Cl_2): δ 8.89 (dd, 1H, J_1 = 5.3 Hz, J_2 = 1.2 Hz, *H*-C═N B[*h*]Q), 8.36 (dd, 1H, J_1 = 8.0 Hz, J_2 = 1.1 Hz, H_{Ar} B[*h*]Q), 8.01 (dd, 1H, J_1 = 6.9 Hz, J_2 = 0.9 Hz, H_{Ar} B[*h*]Q), 7.92 (d, 1H, J = 8.7 Hz, H_{Ar} B[*h*]Q), 7.73 (m, 9H, 1H_{Ar} in B[*h*]Q + 8H_{ortho} in BArF$_{24}$), 7.67−7.70 (m, 2H, H_{Ar} B[*h*]Q), 7.56 (m, 4H_{para} in BArF$_{24}$), 7.61 (dd, 1H, J_1 = 7.9 Hz, J_2 = 5.3 Hz, H_{Ar} B[*h*]Q), 2.12 (s, 3H, Ir-NC*Me*), 1.73 (s, 15H, Cp-*Me*$_5$). ^{13}C NMR (126 MHz, 298 K, CD_2Cl_2): δ 161.5−162.7 (1:1:1:1 quartet, $^1J_{C-B}$ = 49.8 Hz, *C*−B in BArF$_{24}$), 157.6 (*C*-N, B[*h*]Q), 154.2 (CB[*h*]Q), 150.2 (H-C═N, B[*h*]Q), 142.3 (B[*h*]Q), 138.4 (*C*−H, B[*h*]Q), 135.2 (m, *C*−H_{ortho} in BArF$_{24}$), 134.8 (B[*h*]Q), 133.1 (*C*−H, B[*h*]Q), 131.4 (*C*−H, B[*h*]Q), 130.6 (*C*−H, B[*h*]Q), 128.9−129.6 (q, $^2J_{C-F}$ = 31.5 Hz, $^3J_{C-B}$ = 3.0 Hz, *C*-CF_3 in BArF$_{24}$), 128.1 (B[*h*]Q), 125.0 (q, $^1J_{C-F}$ = 272.5 Hz, *C*F$_3$ in BArF$_{24}$), 124.1 (*C*−H, B[*h*]Q), 122.9 (*C*−H, B[*h*]Q), 122.5 (*C*−H, B[*h*]Q), 118.5 (Ir−NCMe), 117.9 (m, *C*−H_{para} in BArF$_{24}$), 91.6 (*Cp*-Me$_5$), 9.1 (Cp-*Me*$_5$), 4.2 (Ir-NC*Me*). ^{19}F NMR (282 MHz, 298 K, CD_2Cl_2): δ −63.8 (s, C*F*$_3$ in BArF$_{24}$). ^{11}B NMR (128 MHz, 298 K, CD_2Cl_2): δ −6.6 (bs). HRMS-ESI: calcd for $C_{25}H_{26}IrN_2$ ([**3b**]$^+$) (*m*/*z*) 547.1721, found 547.1716. HRMS-ESI: calcd for $C_{32}H_{12}BF_{24}$ ([BArF$_{24}$]$^-$) (*m*/*z*) 863.0649, found 863.0656.

*[Cp*Ir(B[h]Q)(NCMe)][BPh$_4$] ([**3b**][BPh$_4$])* (Scheme 2). This compound was prepared following the general procedure described above: **2b** (200 mg, 0.37 mmol), Na[BPh$_4$] (126 mg, 0.37 mmol), MeCN (10 mL), 40 °C, 24 h. After recrystallization from a mixture of CH_2Cl_2 and *n*-pentane the resulting powder was washed with *n*-pentane and dried under reduced pressure to afford [**3b**][BPh$_4$] as a yellow powder in 78% yield (244 mg). Single crystals were grown by slow diffusion of hexane and benzene into a solution of [**3b**][BPh$_4$] in 1,2-dichloroethane. Anal. Calcd for $C_{49}H_{46}BIrN_2 \cdot 1/3CH_2Cl_2$: C, 66.26; H, 5.26; N, 3.13. Found: C, 66.49; H, 5.24; N, 2.96. ^{1}H (500 MHz, 298 K, CD_2Cl_2): δ 8.87 (dd, 1H, J_1 = 5.3 Hz, J_2 = 1.2 Hz, H_{Ar} B[*h*]Q), 8.31 (dd, 1H, J_1 = 8.0 Hz, J_2 = 1.1 Hz, H_{Ar} B[*h*]Q), 8.01 (dd, 1H, J_1 = 7.1 Hz, J_2 = 0.8 Hz, H_{Ar} B[*h*]Q), 7.93 (d, 1H, J = 8.8 Hz, H_{Ar} B[*h*]Q), 7.74 (d, 1H, J = 7.8 Hz, H_{Ar} B[*h*]Q), 7.69 (t, 2H, J = 7.0 Hz, H_{Ar} B[*h*]Q), 7.26 (m, 9H, 1H_{Ar} in B[*h*]Q + 8H_{Ar} in BPh$_4$), 6.95 (t, 8H, J = 7.2 Hz, H_{Ar} in BPh$_4$), 6.82 (m, 4H, H_{Ar} in BPh$_4$), 1.74 (s, 3H, Ir-NC*Me*), 1.59 (s, 15H, Cp-*Me*$_5$). ^{13}C NMR (126 MHz, 298 K, CD_2Cl_2): δ 164.5 (1:1:1:1 quartet, $^1J_{C-B}$ = 49.2 Hz, *C*−B in BPh$_4$), 157.5 (B[*h*]Q), 154.3 (B[*h*]Q), 150.2 (H-*C*=N, B[*h*]Q), 142.3 (B[*h*]Q), 138.5 (H-*C*, B[*h*]Q), 136.2 (1:1:1:1 quartet, $^3J_{C-B}$ = 1.4 Hz, *C*−H_{ortho} in BPh$_4$), 134.8 (B[*h*]Q), 133.1 (*C*−H, B[*h*]Q), 131.4 (*C*−H, B[*h*]Q), 130.6 (*C*−H, B[*h*]Q), 128.7 (B[*h*]Q), 126.0 (1:1:1:1 quartet, $^2J_{C-B}$ = 2.8 Hz, *C*−H_{meta} in BPh$_4$), 124.2 (*C*−H, B[*h*]Q), 123.1 (*C*−H, B[*h*]Q), 122.5 (*C*−H, B[*h*]Q), 122.1 (s, *C*−H_{para} in BPh$_4$), 119.0 (Ir−NCMe), 91.5 (*Cp*-Me$_5$), 9.2 (Cp-*Me*$_5$), 3.4 (Ir-NC*Me*). ^{11}B (128 MHz, 298 K, $CDCl_3$): δ −6.5 (m). HRMS-ESI: calcd for $C_{25}H_{26}IrN_2$ ([**3b**]$^+$) (*m*/*z*) 547.1721, found 547.1758. HRMS-ESI: calcd for $C_{24}H_{20}B$ ([BPh$_4$]$^-$) (*m*/*z*) 319.1657, found 319.1655.

*[Cp*Ir(B[h]Q)(NCMe)][OTf] ([**3b**][OTf])* (Scheme 2). This compound was prepared following the general procedure described above: **2b** (93.5 mg, 0.173 mmol), Ag[OTf] (342.2 mg, 0.173 mmol), MeCN (7 mL), room temperature, 2 h. After the resulting residue was washed with *n*-pentane, [**3b**][OTf] was recovered as a yellow powder in 76% yield (113 mg). Anal. Calcd for $C_{26}H_{26}F_3IrN_2O_3S \cdot 1/10CH_2Cl_2$: C, 44.51; H, 3.75; N, 3.98. Found: C, 44.81; H, 3.77; N, 4.03. ^{1}H (400 MHz, 298 K, $CDCl_3$): δ 9.26 (d, 1H, J = 5.3 Hz, H−C═N B[*h*]Q), 8.32 (d, 1H, J = 8.1 Hz, H_{Ar} B[*h*]Q), 7.97 (d, 1H, J = 6.7 Hz, H_{Ar} B[*h*]Q), 7.87 (d, 1H, J = 8.8 Hz, H_{Ar} B[*h*]Q), 7.77 (dd, 1H, J_1 = 8.0 Hz, J_2 = 8.0 Hz, H_{Ar} B[*h*]Q), 7.63−7.70 (m, 3H, H_{Ar} B[*h*]Q), 2.28 (s, 3H, Ir-NC*Me*), 1.79 (s, 15H, Cp-*Me*$_5$). ^{13}C (126 MHz, 298 K, $CDCl_3$): δ 156.8 (B[*h*]Q), 154.4 (B[*h*]Q), 151.6 (*C*−H, B[*h*]Q), 142.1 (B[*h*]Q), 137.7 (*C*−H, B[*h*]Q), 134.2 (B[*h*]Q), 132.7 (*C*−H, B[*h*]Q), 130.7 (*C*−H, B[*h*]Q), 129.9 (*C*−H, B[*h*]Q), 127.3 (B[*h*]Q), 123.9 (*C*−H, B[*h*]Q), 123.3 (*C*−H, B[*h*]Q), 121.9 (*C*−H, B[*h*]Q), 119.0 (Ir−NCMe), 91.1 (*Cp*-Me$_5$), 9.0 (Cp-*Me*$_5$), 4.1 (Ir-NC*Me*). ^{19}F{^{1}H} (282 MHz, 298 K, $CDCl_3$): δ −78.9 (C*F*$_3$, OTf). HRMS-ESI (*m*/*z*): calcd for $C_{25}H_{26}IrN_2$ ([**3b**]$^+$) 547.1721, found 547.1655. HRMS-ESI (*m*/*z*): calcd for CF_3O_3S ([OTf]$^-$) 148.9515, found 148.9530.

*[Cp*Ir(B[h]Q)(NCMe)][BArF$_{20}$] ([**3b**][BArF$_{20}$])* (Scheme 2). This compound was prepared following the general procedure described above: **2b** (200 mg, 0.370 mmol), K[BArF$_{20}$] (264 mg, 0.368 mmol), MeCN (7 mL), room temperature, 2 h. After recrystallization from a mixture of CH_2Cl_2 and *n*-pentane the resulting powder was washed with *n*-pentane and dried under reduced pressure to afford [**3b**][BArF$_{20}$] as a yellow powder in 86% yield (387 mg). Single crystals were grown by slow diffusion of hexane into a solution of [**3b**][BArF$_{20}$] in dichloromethane (−30 °C). Anal. Calcd for $C_{49}H_{26}BF_{20}IrN_2 \cdot CH_2Cl_2$: C, 45.82; H, 2.15; N, 2.14. Found: C, 45.96; H, 1.99; N, 2.38. ^{1}H NMR (400 MHz, 298 K, CD_2Cl_2): δ 8.91 (dd, 1H, J_1 = 5.4 Hz, J_2 = 1.3 Hz, H−C═N B[*h*]Q), 8.39 (dd, 1H, J_1 = 8.0 Hz, J_2 = 1.4 Hz, H_{Ar} B[*h*]Q), 8.02 (dd, 1H, J_1 = 6.9 Hz, J_2 = 1.3 Hz, H_{Ar} B[*h*]Q), 7.93 (d, 1H, J = 8.8 Hz, H_{Ar} B[*h*]Q), 7.74 (dd, 1H, J_1 = 7.9 Hz, J_2 = 1.2 Hz, H_{Ar} B[*h*]Q), 7.72−7.66 (m, 2H, H_{Ar} B[*h*]Q), 7.63 (dd, 1H, J_1 = 8.1 Hz, J_2 = 5.3 Hz, H_{Ar} B[*h*]Q), 2.15 (s, 3H, Ir-NC*Me*), 1.75 ppm (s, 15H, Cp-*Me*$_5$). ^{13}C NMR (126 MHz, 295 K, CD_2Cl_2): δ 158.0 (*C*-N, B[*h*]Q), 154.7 (B[*h*]Q), 150.6 (H-C═N, B[*h*]Q), 148.9 (*C*-F, d (br), ^1J = 240.0 Hz, 2C of C_6F_5 in BArF$_{20}$), 142.7 (B[*h*]Q), 138.8 (*C*-F, d (br), ^1J = 240.0 Hz, 1C of *p*-C_6F_5 in BArF$_{20}$), 138.8 (*C*−H, B[*h*]Q), 136.2 (*C*−F, d (br), ^1J = 240.0 Hz, 2C of C_6F_5 in BArF$_{20}$), 135.3 (B[*h*]Q), 133.6 (*C*−H, B[*h*]Q), 131.8 (*C*−H, B[*h*]Q), 131.0 (*C*−H, B[*h*]Q), 128.5 (B[*h*]Q), 124.5 (*C*−H, B[*h*]Q), 123.3 (*C*−H, B[*h*]Q), 122.9 (*C*−H, B[*h*]Q), 119.0 (Ir−NCMe), 92.1 (*Cp*-Me$_5$), 9.6 (Cp-*Me*$_5$), 4.6 (Ir−NC*Me*), [the 1:1:1:1 quartet characterizing the *C*-B bond in C_6F_5 (BArF$_{20}$) escaped detection]. ^{11}B NMR (128 MHz, 298 K, CD_2Cl_2): δ −16.6 (s). HRMS-ESI: calcd for $C_{23}H_{23}IrN$ ([**3b** - NCMe]$^+$) (*m*/*z*) 506.1455, found 506.1462.

*[Cp*Ir(DB[f,h]Q)(NCMe)][BArF$_{24}$] ([**3c**][BArF$_{24}$])* (Scheme 2). This compound was prepared following the general procedure described above: **2c** (100 mg, 0.169 mmol), Na[BArF$_{24}$] (150.0 mg, 0.169 mmol), MeCN (10 mL), 50 °C, 5 h. After recrystallization with a mixture of CH_2Cl_2 and *n*-pentane (∼−30 °C) the resulting powder was washed with *n*-pentane and dried under reduced pressure to afford [**3c**][BArF$_{24}$] as an orange-yellow powder in 70% yield (172 mg). Anal. Calcd for $C_{61}H_{40}BF_{24}IrN_2 \cdot 4/5CH_2Cl_2$: C, 48.58; H, 2.74; N, 1.83. Found: C, 48.22; H, 2.70; N, 1.59. ^{1}H (500 MHz, 298 K, d_6-acetone): δ 9.33 (d, 1H, J = 8.3 Hz, H_{Ar} DB[*f*,*h*]Q), 9.28 (d, 1H, J = 5.5 Hz, H_{Ar} DB[*f*,*h*]Q), 8.86 (t, 2H, J = 7.6 Hz, H_{Ar} DB[*f*,*h*]Q), 8.46 (d, 1H, J = 8.0 Hz, H_{Ar} DB[*f*,*h*]Q), 8.13 (d, 1H, J = 7.3 Hz, H_{Ar} DB[*f*,*h*]Q), 7.85−7.91 (m, 2H, H_{Ar} DB[*f*,*h*]Q), 7.79 (m; 1H_{Ar} in DB[*f*,*h*]Q + 8H_{ortho} in BArF$_{24}$), 7.73 (t, 1H, J = 7.5 Hz, H_{Ar} DB[*f*,*h*]Q), 7.68 (m, 4H_{para} in BArF$_{24}$), 2.41 (s, 3H, Ir-NC*Me*), 1.86 (s, 15H, Cp-*Me*$_5$). ^{13}C NMR (126 MHz, 298 K, d_6-acetone): δ 162.6 (1:1:1:1 quartet, $^1J_{C-B}$ = 49.6 Hz, *C*-B in BArF$_{24}$), 158.7 (DB[*f*,*h*]Q), 156.3 (DB[*f*,*h*]Q), 152.4 (H-*C*=N, DB[*f*,*h*]Q), 141.3 (DB[*f*,*h*]Q), 135.5 (*C*−H, DB[*f*,*h*]Q), 134.6 (*C*−H, DB[*f*,*h*]Q), 134.6 (*C*−H, DB[*f*,*h*]Q), 133.1 (DB[*f*,*h*]Q), 132.2 (m, DB[*f*,*h*]Q), 130.4 (*C*−H, DB[*f*,*h*]Q), 130.1 (*C*−H, DB[*f*,*h*]Q), 130.0 (q, $^2J_{C-F}$ = 32.3 Hz, *C*-CF_3 in BArF$_{24}$), 128.8 (*C*−H, DB[*f*,*h*]Q), 128.7 (DB[*f*,*h*]Q), 127.4 (DB[*f*,*h*]Q), 125.4 (q, $^1J_{C-F}$ = 271.5 Hz, *C*F$_3$ in BArF$_{24}$), 125.0 (*C*−H, DB[*f*,*h*]Q), 124.9 (*C*−H, DB[*f*,*h*]Q), 124.4 (*C*−H, DB[*f*,*h*]Q), 118.4 (m, *C*−H_{para} in BArF$_{24}$), 118.3 (Ir−NCMe), 92.3 (*Cp*-Me$_5$), 10.0 (Cp-*Me*$_5$), 3.4 (Ir-NC*Me*). ^{19}F{^{1}H} NMR (282 MHz, 298 K, d_6-acetone): δ −64.2 (s, C*F*$_3$ in BArF$_{24}$). ^{11}B NMR (128 MHz, 298 K, d_6-acetone): δ −6.54 (m). HRMS-ESI: calcd for $C_{29}H_{28}IrN_2$ ([**3c**]$^+$) (*m*/*z*) 597.1887, found 597.1914. HRMS-ESI: calcd for $C_{32}H_{12}BF_{24}$ ([BArF$_{24}$]$^-$) (*m*/*z*) 863.0649, found 863.0649.

Procedure for Piezometric Monitoring of the Catalytic *O*-Silylation of Benzyl Alcohol (eq 1, Table 2). Benzyl alcohol (1.0 mL, 9.6 mmol or 0.5 mL, 4.8 mmol) and $HSiEt_3$ (0.8 mL, 5.0 mmol)

DOI: 10.1021/acs.organomet.7b00749
Organometallics XXXX, XXX, XXX−XXX

were introduced in a small-volume double-walled Schlenk vessel (~28 mL) thermostated at 20 °C. After the resulting mixture was slowly stirred for a few minutes, a Mykrolis A332984−007 absolute pressure-to-voltage transducer was airtightly screwed to the neck of the glass vessel and connected to a Pico-Log analog−logic converter/data-logger board interfaced to a computer. This allowed the measurement of the pressure of hydrogen (computed from a linear absolute pressure−output voltage relationship) developed in the known overhead volume of the sealed reactor as a function of time. The absence of leaks was preliminarily checked by applying a moderate pressure of argon gas. The iridium precatalyst ([**3a**][$BArF_{24}$], 6.7 or 6.9 mg, 4.8 or 5.0 μmol; [**3b**][$BArF_{24}$], 6.2 mg, 4.4 μmol; [**3c**][$BArF_{24}$],7.0 mg, 4.8 μmol; [**3a**][$BArF_{20}$], 5.8 mg, 4.8 μmol; [**3b**][$BArF_{20}$], 5.9 mg, 4.8 μmol; 0.1 mol % relative to $HSiEt_3$) dissolved in 1,2-dichloroethane (0.5 mL) was swiftly injected into the vessel via a lateral glass valve, which was tightly closed immediately upon injection to avoid gas leaks. A blank control experiment carried out without any precatalyst did not produce any noticeable hydrogen gas pressure. A picture of the setup used here is given in Figure S31 in the Supporting Information.

General Procedures for the Catalytic Hydrosilylation of Acetonitrile and Propionitrile (Table 3). *Procedure 1 (Solvent-Free Conditions, Entries 1−5).* To a solution of [**3a**][$BArF_{24}$] or [**3b**][$BArF_{24}$] (0.1 or 1 mol %) in MeCN (0.5 or 1 mL, 9.7 or 19.4 mmol) was added $HSiEt_3$ (3.1 or 6.73 mL, 19.4 or 42.1 mmol). The reaction mixture was heated at the given temperature for the given time. The reaction mixture was monitored using ^{1}H NMR spectroscopy at different intervals of time. After 44 h of reaction at 50 °C (entry 2), the temperature of the reaction mixture was raised to 100 °C (entry 3). For ^{1}H NMR spectroscopy analysis, tri-*tert*-butylbenzene was added as an internal reference to the reaction mixture, after which an aliquot was taken from this mixture and mixed with CD_2Cl_2 or C_6D_6. For spectroscopic details, see the Supporting Information.

Procedure 2 (with CH_2Cl_2 as the Solvent, Entries 6−13). To a solution of alkylnitrile (1 equiv) and silane (2.2 equiv) was added [**3b**][$BArF_{24}$] (0.1 or 1 mol %) in CH_2Cl_2 (0.5 mL). The reaction mixture was heated at either 60 °C for 72 h (entry 6) or at 80 °C for 24 h (entries 7−13). For ^{1}H NMR analyses, tri-*tert*-butylbenzene was added as an internal reference to the reaction mixture, after which an aliquot was taken from this mixture and mixed with C_6D_6. For spectroscopic details, see the Supporting Information.

*Data for **9H$_2$** and Its Tautomer **9′H$_2$** (from Fraction 1) (Figure 3).* Anal. Calcd for $C_4H_{10}N_2$: C, 55.78; H, 11.70; N, 32.52. Found: C, 54.34; H, 11.31; N, 31.71. ^{1}H NMR (500 MHz, 298 K, $CDCl_3$): δ 3.16 (q, 2H, J = 7.0 Hz, $-CH_2-$), 1.94 (s, 3H, $CH_3-C{=}N-$), 1.16 (t, 3H, J = 7.1 Hz, CH_3-CH_2-). ^{13}C NMR (126 MHz, 298 K, $CDCl_3$): δ 161.3 (−C═N−, because not directly visible, its presence was inferred from ^{1}H,^{13}C HMBC 2D-correlation spectrum), 36.7 ($-CH_2-$), 23.9 ($CH_3-C{=}N-$), 14.8 (CH_3-CH_2-).

*Data for **10H$_2$** (from Fraction 2).* The sample was obtained as a mixture with **9H$_2$** in a respective ratio of ~0.8:1. ^{1}H NMR (500 MHz, 298 K, $CDCl_3$): δ 3.25 (q, 2H, J = 7.3 Hz, $-CH_2-$), 2.00 (s, 6H, $CH_3-C{=}N-$), 1.11 (t, 3H, J = 7.3 Hz, CH_3-CH_2-). ^{13}C NMR (126 MHz, 298 K, $CDCl_3$): δ 172.5 (−C═N−), 34.5 ($-CH_2-$), 22.7 ($CH_3-C{=}N-$), 15.0 (CH_3-CH_2-).

General Procedures for the Catalytic Hydrosilylation of Benzonitrile (Table 4). *Procedure 1 (Solvent-Free Conditions, Entries 1 and 2).* To a solution of [**3a**][$BArF_{24}$] (135 mg, 97 μmol, 1 mol %) in benzonitrile (1 mL, 9.7 mmol) was added $HSiEt_3$ (3.1 mL, 19.5 mmol). The reaction mixture was heated at 50 °C for 20 h (entry 1) and then at 80 °C for 24 h (entry 2). The reaction mixture was monitored using ^{1}H NMR spectroscopy at these two intervals of time. For each analysis, tri-*tert*-butylbenzene was added as internal reference to the reaction mixture, after which an aliquot from the reaction mixture was taken and mixed with CD_2Cl_2 for NMR analysis. For spectroscopic details, see the Supporting Information.

Procedure 2 (with CH_2Cl_2 as the Solvent, Entries 3−8). To a mixture of benzonitrile (1 equiv) and $HSiEt_3$ (2.2 equiv) was added a solution of [**3b**][$BArF_{24}$] (0.001−1 mol %) in CH_2Cl_2 (0.5 mL). The reaction mixture was heated at the given temperature for the given time. For ^{1}H NMR analysis, tri-*tert*-butylbenzene was added as internal reference to the reaction mixture, after which an aliquot was taken from this mixture and mixed with CD_2Cl_2 or C_6D_6. For further details, see the Supporting Information.

General Procedure for the [3b][$BArF_{24}$] Load Optimization in the Catalytic Hydrosilylation of Benzonitrile with $HSiEt_3$ (Figure 5). Using the general procedure described above (Table 4), the conditions for each catalytic run were as follows: benzonitrile (0.1 mL, 0.97 mmol), $HSiEt_3$ (0.35 mL, 2.13 mmol), [**3b**][$BArF_{24}$] (0.48 μmol, 0.05 mol %; 0.1 μmol, 0.1 mol %; 1.9 μmol, 0.2 mol %; 4.8 μmol, 0.5 mol %; 9.7 μmol, 1 mol %), CH_2Cl_2 (0.5 mL). The reaction progress was monitored at different times by using ^{1}H NMR spectroscopy. For further details, see Table S2 in the Supporting Information.

Reaction of [3b][$BArF_{24}$] with $HSiEt_3$ (Step 1, Scheme 3). In a glovebox, $HSiEt_3$ (~10 μL, 62.6 μmol) was added to a solution of [**3b**][$BArF_{24}$] (20 mg, 14.2 μmol) in CD_2Cl_2 (0.55 mL) placed in a vial equipped with a septum. The resulting solution was vigorously shaken and transferred into a J. Young NMR sample tube, which was subsequently tightly sealed for analysis. After ~25 min the NMR tube was frozen and introduced in the NMR spectrometer's probe. Multinuclear NMR analysis (at −60 °C) of the reaction mixture revealed the total conversion of [**3b**][$BArF_{24}$] into mainly [**4b**][$BArF_{24}$], [**7b**][$BArF_{24}$], and $EtN(Et_3Si)_2$ along with unconsumed $HSiEt_3$ in a respective ratio of ~1:0.1:1.2:1.2 (see spectra in the Supporting Information). Data for [**4b**][$BArF_{24}$] are as follows. ^{1}H NMR (600 MHz, 213 K, CD_2Cl_2): δ 8.67 (d, 1H, J = 5.3 Hz, H_{Ar} B[*h*]Q), 8.38 (d, 1H, J = 8.0 Hz, H_{Ar} B[*h*]Q), 7.90 (d, 1H, J = 8.8 Hz, H_{Ar} B[*h*]Q), 7.8 (t, 2H, J = 7.4 Hz, H_{Ar} B[*h*]Q), 7.73 (m, 8H, H_{ortho} $BArF_{24}$), 7.70 (t, 1H, J = 8.3 Hz, H_{Ar} B[*h*]Q), 7.71 (m, 1H, H_{Ar} B[*h*]Q), 7.67 (d, 1H, J = 8.7 Hz, H_{Ar} B[*h*]Q), 7.59 (dd, 1H, J_1 = 7.9 Hz, J_2 = 7.9 Hz, H_{Ar} B[*h*]Q), 7.53 (s, 4H, H_{para} $BArF_{24}$), 1.69 (s, 15H, Cp-Me_5), 0.56 (t, 9H, J = 7.9 Hz, [Ir]-Si(CH_2CH_3)$_3$), 0.29 (m, 3H [Ir]-Si(CH_2CH_3)$_3$), 0.22 (m, 3H, [Ir]-Si(CH_2CH_3)$_3$), − 11.44 (bs, 1H, J_{H-Si} = 20 Hz, [Ir]-*H*). The reaction described above was repeated again for recording of the ^{13}C spectrum (and additional 2D ^{1}H,^{13}C spectra): ^{13}C NMR (126 MHz, 300 K, CD_2Cl_2): δ 161.5 (1:1:1:1 quartet, $^1J_{C-B}$ = 49.6 Hz, *C*-B in $BArF_{24}$), 156.5 (B[*h*]Q), 151.5 (H−*C*═N, B[*h*]Q), 143.9 (B[*h*]Q), 140.8 (B[*h*]Q), 138.6 (*C*−H, B[*h*]Q), 135.0 (B[*h*]Q), 134.9 (*C*−H, B[*h*]Q), 134.4 (s, *C*−H_{ortho} in $BArF_{24}$), 130.3 (*C*−H, B[*h*]Q), 130.2 (*C*−H, B[*h*]Q), 128.4 (q, $^2J_{C-F}$ = 30.6 Hz, *C*-CF_3 in $BArF_{24}$), 128.1 (B[*h*]Q), 124.2 (q, $^1J_{C-F}$ = 272.8 Hz, CF_3 in $BArF_{24}$), 124.0 (*C*−H, B[*h*]Q), 123.3 (*C*−H, B[*h*]Q), 122.7 (*C*−H, B[*h*]Q), 117.3 (m, *C*−H_{para} in $BArF_{24}$), 101.3 (*Cp*-Me_5), 8.8 (Cp-Me_5), 8.6 ([Ir]-Si(CH_2CH_3)$_3$), 5.8 ([Ir]-Si(CH_2CH_3)$_3$), 5.3 ([Ir]-Si(CH_2CH_3)$_3$). ^{29}Si-DEPT NMR (119 MHz, 213 K, CD_2Cl_2): δ 6.93 (s, [Ir]-*Si*Et_3), 6.90 (s, [Ir]-*Si*Et_3). Data for $EtN(Et_3Si)_2$ are as follows: ^{1}H NMR (600 MHz, 213 K, CD_2Cl_2): δ 2.81 (q, 2H, J = 7.0 Hz, N−CH_2CH_3), 0.98 (t, 3H, J = 7.0 Hz, N−CH_2CH_3), 0.90 (t, 18H, J = 8.0 Hz, $SiCH_2CH_3$), 0.56 (q, 12H, J = 8.0 Hz, $SiCH_2CH_3$,). ^{29}Si-DEPT NMR (119 MHz, 213 K, CD_2Cl_2): δ 10.9 ($(Et_3Si)_2NEt$). Data for unconsumed and "free" $HSiEt_3$ are as follows. ^{1}H NMR (600 MHz, 213 K, CD_2Cl_2): δ 3.50 (sept, 1H, $^1J_{H-Si}$ = 173.6 Hz, *H*−$SiEt_3$), 0.89 (t, 9H, J = 8.0 Hz, $SiCH_2CH_3$,), 0.52 (q, 6H, J = 8.0 Hz, $SiCH_2CH_3$,). ^{29}Si-DEPT NMR (119 MHz, 213 K, CD_2Cl_2): δ 0.0 (s, H*Si*Et_3). A ^{29}Si signal of significant intensity (see ^{1}H−^{29}Si HMQC and ^{29}Si-DEPT spectra in the Supporting Information) at δ 9.5 ppm (s) could not be assigned with certainty to any known molecule or side product of the acetonitrile hydrosilylation.

Procedure for the Attempted in Situ Generation of [$Et_3Si(NCMe)_n$][OTf] Followed by Its Stoichiometric Reaction with either $HSiEt_3$ or 5b (Step 3, Scheme 3). MeCN (2.5 μL, 126 μmol) was added to a solution of TfO-$SiEt_3$ (14 μL, 63 μmol) in CD_2Cl_2 (~0.5 mL) placed in a 2 mL vial equipped with a septum. The reaction mixture was vigorously shaken at room temperature for a few seconds and subsequently transferred into a J. Young NMR sample tube that was then tightly sealed. The NMR tube was subsequently put in the probe of the spectrometer (set at 25 °C) for spectral acquisition. The resulting ^{1}H NMR spectrum showed the presence of the characteristic peaks of both free acetonitrile (δ 1.99 (bs)) and free

DOI: 10.1021/acs.organomet.7b00749
Organometallics XXXX, XXX, XXX−XXX

TfO-$SiEt_3$ (δ 1.09 (t, 9H, J = 8.0 Hz, CH_3CH_2Si−); 0.97 (q, 6H, J = 8.0 Hz, CH_3CH_2Si)). The NCMe:TfO-$SiEt_3$ ratio was estimated to be ∼2:1. To this solution mixture was then added a CD_2Cl_2 solution (∼0.2 mL) of either $HSiEt_3$ (10 μL, 62.6 μmol) or **5b** (32 mg, 63.2 μmol). The resulting solution was shaken at room temperature for a few seconds before a new NMR spectrum was recorded. In the case of the experiment run with $HSiEt_3$, the resulting NMR spectrum showed no noticeable change in the characteristic chemical shifts of respectively free MeCN, TfO-$SiEt_3$, and $HSiEt_3$. However, in the case of the experiment run with **5b**, the resulting NMR spectrum showed quantitative conversion of **5b** to new iridium species. Among the latter, the ionic salt [**3b**][OTf] was found to be the major iridium species on the basis of the identification of its typical signals in comparison to those of an authentic sample. While the typical signals of TfO-$SiEt_3$ were no longer detected, typical signals of free MeCN and coordinated MeCN ([**3b**][OTf]) were observed respectively at δ 1.99 ppm (bs) and δ 2.19 ppm (s). Finally, characteristic peaks of the products of hydrosilylation of acetonitrile were not observed. Although typical signals of the ethyl moiety were indeed observed at δ 0.94 ppm (t, 9H) and δ 0.53 ppm (q, 6H)), the fate of the silylium cation $[SiEt_3]^+$ could not be traced.

Procedure for the in Situ Generation of $[Et_3Si(NCMe)_n][BArF_{20}]$ Followed by Its Stoichiometric Reaction with 5b (Step 3, Scheme 3; Scheme 5). In a 2 mL vial equipped with a septum, MeCN (2.5 μL, 48.7 μmol) was added to a solution of $[Ph_3C][BArF_{20}]$ (10.0 mg, 10.8 μmol) in CD_2Cl_2 (∼0.5 mL). The reaction mixture was cooled to 0 °C and transferred into a J. Young NMR sample tube, which was subsequently tightly sealed. The NMR tube was left at 0 °C for ∼15 min before recording the first ^{1}H NMR spectrum (the spectrometer's probe temperature was set to 0 °C). The resulting ^{1}H NMR spectrum revealed characteristic peaks of both MeCN (δ 1.99 (bs)) and $[Ph_3C][BArF_{20}]$ (δ 8.25 (t, 3H, J = 7.4 Hz, H_{para}); 7.86 (t, 6H, J = 7.4 Hz, H_{meta}); 7.66 (d, 6H, J = 7.6 Hz, H_{ortho})) accompanied by some residual acetone impurity (δ 2.13 (bs)) in a respective ratio of 4:1:0.3 (see the NMR spectra in the Supporting Information). To this solution mixture was subsequently added $HSiEt_3$ (3.5 μL, 22 μmol). The resulting orange solution was shaken at 0 °C for a few seconds before a new NMR analysis was recorded. The resulting NMR spectrum showed the quantitative conversion of $[Ph_3C][BArF_{20}]$ and MeCN into respectively Ph_3CH (^{1}H: δ 7.29 (t, 6H, J = 7.3 Hz, H_{meta}); 7.22 (t, 3H, J = 7.3 Hz, H_{para}); 7.12 (d, 6H, J = 7.3 Hz, H_{ortho})), solvated proton, and $O(SiEt_3)_2$ (^{1}H: δ 2.13 (bs, nH, −NC*Me*); 0.93 (t, 9H, CH_3CH_2Si−); 0.52 (q, 6H, CH_3CH_2Si--); ^{29}Si: δ 8.92 (s, Et_3Si−)) accompanied by excess $HSiEt_3$ (^{1}H: δ 3.59 (sept, 1H, J = 3.0 Hz, H−Si−); 0.96 (t, 9H, J = 7.9 Hz, CH_3CH_2Si−); 0.52 (qd, 6H, J_1= 8.0 Hz, J_2 = 3.0 Hz, CH_3CH_2Si−); ^{29}Si: δ 0.53 (s, Et_3Si−)) and the product of hydrosilylation of the residual acetone, i.e. $[CH_3CHO(SiEt_3)]$ (^{1}H: δ 4.71 (sept, 1H, J = 6.2 Hz, CH_3CH−); the signals of the $SiEt_3$ group overlapped with other similar groups). The Ph_3CH:$O(SiEt_3)_2$:$HSiEt_3$:$[CH_3CHO(SiEt_3)]$ ratio was estimated to be ∼1:0.5:0.6:0.5. To this solution mixture was then added a solution of **5b** (5.5 mg, 10.8 μmol) in CD_2Cl_2 (∼0.5 mL). The resulting red solution was shaken at 0 °C for a few seconds before a new NMR analysis was recorded. The resulting NMR spectrum revealed the quantitative conversion of **5b** (^{1}H: δ 1.90 (s, 15H, Cp-Me_5); −15.28 (s, 1H, Ir-*H*)) into [**7b**][$BArF_{20}$] (^{1}H: δ 1.42 (s, 30H, Cp-Me_5); −22.80 (s, 1H, Ir-*H*)) and [**3b**][$BArF_{20}$] (^{1}H: δ 2.13 (s, 3H, Ir-NC*Me*), 1.73 (s, 15H, Cp-Me_5)). The spectrum also revealed the formation of the three main hydrosilylation products $EtNR_2$ (R = $SiEt_3$ H, $N(SiEt_3)C(Me)$=$N(SiEt_3)_2$), as suggested by the presence of the characteristic CH_3CH_2N− quadruplet resonance signal at respectively δ(^{1}H) 3.65 (J = 6.8 Hz); 2.83 (J = 7.0 Hz), and 2.75 (J = 7.0 Hz) (see the NMR spectra in the Supporting Information for details). The chemical shift at δ 2.83 ppm is assigned to the product of double hydrosilylation of MeCN: i.e., $EtN(SiEt_3)_2$. The Ph_3CH:[**7b**][$BArF_{20}$]:[**3b**][$BArF_{20}$]:$EtNR_2$ ratio was estimated to be ∼1.9:1:2.

Procedure for the Crystallization of [{Cp*Ir(B[*h*]Q)}$_2$(μ-H)][$BArF_{24}$] ([7b][$BArF_{24}$]) (Step 5, Scheme 3). Red single crystals of [**7b**][$BArF_{24}$] suitable for X-ray diffraction analysis were grown by slow diffusion of a *n*-hexane/benzene solution of excess $HSiEt_3$ into a solution of [**3b**][$BArF_{24}$] in 1,2-dicholoremethane.

NMR Data for [{Cp*Ir(B[*h*]Q)}$_2$(μ-H)][$BArF_{24}$] ([7b][$BArF_{24}$] and [7b′][$BArF_{24}$]) (Step 5, Scheme 3). Since [**7b**][$BArF_{24}$] and [**7b′**][$BArF_{24}$] could not be successfully isolated, their ^{1}H NMR data were obtained from their in situ formation (in a J. Young NMR sample tube) by reaction of [**3b**][$BArF_{24}$] with **5b** (see the procedure below). ^{1}H NMR data for [**7b**][$BArF_{24}$] (major product) (400 MHz, 298 K, CD_2Cl_2): δ 8.07 (d, 2H, J = 7.3 Hz, H−C=N B[*h*]Q), 7.67−7.75 (m, 4H, H_{Ar} of B[*h*]Q overlapped with H_{ortho} of $BArF_{24}$), 7.54 (d, 2H, H_{Ar} of B[*h*]Q overlapped with H_{para} of $BArF_{24}$), 7.36 (dd, 2H, J_1 = 6.9 Hz, J_2 = 1.9 Hz, H_{Ar} B[*h*]Q), 7.28 (d, 1H, J = 8.8 Hz, H_{Ar} B[*h*]Q), 6.10−6.13 (m, 4H, H_{Ar} B[*h*]Q), 1.43 (s, 30H, Cp-Me_5), −22.63 (s, 1H, Ir-*H*). ^{1}H NMR data for [**7b′**][$BArF_{24}$] (minor product) (400 MHz, 298 K, CD_2Cl_2): δ 7.77 (m, 2H, H−C=N H_{Ar} of B[*h*]Q overlapped with H_{para} of $BArF_{24}$), 7.41 (d, 2H, J = 8.7 Hz, H_{Ar} B[*h*]Q), 7.25 (d, 2H, H_{Ar} of B[*h*]Q overlapped with H_{para} of $BArF_{24}$), 7.01 (t, 2H, J = 7.5 Hz, H_{Ar} B[*h*]Q), 6.86 (dd, 2H, J_1 = 8.0 Hz, J_2 = 8.0 Hz, H_{Ar} B[*h*]Q), 6.78 (d, 2H, J = 7.3 Hz, H_{Ar} B[*h*]Q), 6.10−6.13 (m, 4H, H_{Ar} B[*h*]Q), 1.43 (s, 30H, Cp-Me_5), −22.79 (s, 1H, Ir-*H*).

Reaction of [3a][$BArF_{24}$] with 5a (Step 5, Scheme 3; Scheme 6). In a glovebox, a solution of [**3a**][$BArF_{24}$] (35.9 mg, 25.9 μmol) in CD_2Cl_2 (∼0.6 mL) was placed in a vial containing **5a** (5.0 mg, 10.4 μmol). The resulting red solution was shaken at room temperature for few seconds and transferred into a J. Young NMR sample tube, which was tightly sealed. The NMR tube was left at room temperature for 15 min before recording the ^{1}H NMR spectrum. The NMR tube was subsequently left to stand for ∼2.5 h at room temperature before excess MeCN (53 μL, 1.04 mmol) was added. After 15 min, a new NMR spectrum was recorded. See the Supporting Information for assigned NMR spectra.

Reaction of [3b][$BArF_{24}$] with 5b (Step 5, Scheme 3; Scheme 6). In a glovebox, a solution of [**3b**][$BArF_{24}$] (18.1 mg, 13 μmol) in CD_2Cl_2 (∼0.3 mL) was placed in a vial containing a solution of **5b** (5.0 mg, 10 μmol) in CD_2Cl_2 (∼0.3 mL). The resulting red solution was shaken at room temperature for a few seconds and transferred into a J. Young NMR sample tube, which was tightly sealed. The NMR tube was left to stand at room temperature for 15 min before recording the ^{1}H NMR spectrum. The NMR tube was subsequently left to stand for ∼4 h at room temperature before excess MeCN (25 μL, 774.0 μmol) was added. After 15 min, a new NMR spectrum was recorded. See the Supporting Information for assigned NMR spectra.

Reaction of [Ph_3C][$BArF_{20}$] with 5a (Step 5, Scheme 3; eq 3). In a glovebox, a solution of $[Ph_3C][BArF_{20}]$ (9.5 mg, 10.4 μmol) in d_5.PhCl (∼0.3 mL) was placed in a vial containing a solution of **5a** (10 mg, 20.7 μmol) in d_5-PhCl (∼0.3 mL). The resulting red solution was shaken at room temperature for a few seconds and transferred into a J. Young NMR sample tube, which was tightly sealed. The NMR tube was left to stand at room temperature for 15 min before recording the ^{1}H NMR spectrum. The resulting ^{1}H NMR spectrum showed quantitative conversion of the starting material into Ph_3CH and **7a**. See the Supporting Information for the assigned NMR spectrum.

Procedure for ^{1}H and ^{2}H NMR Monitoring of the Catalytic Hydrosilylation of CD_3CN Catalyzed by [3a][$BArF_{24}$] (Steps 3 and 5, Scheme 3). This experiment was first conducted at room temperature and then repeated at −50 °C, as described by the following general procedure: in a glovebox, CD_3CN (9.2 μL, 180 μmol) was added to a solution of [**3a**][$BArF_{24}$] (25 mg, 18 μmol) in CD_2Cl_2 (0.5 mL) placed in a vial equipped with a septum. $HSiEt_3$ (58 μL, 360 μmol) was then added dropwise. The resulting solution was shaken and transferred into a J. Young NMR sample tube, which was subsequently tightly sealed for analysis. After 30 min of reaction at room temperature (or 60 min at −50 °C), the NMR tube was introduced in the NMR spectrometer's probe (298 or 223 K). ^{1}H and ^{2}H NMR spectra were subsequently recorded (see spectra in Supporting Information).

Procedure for the Catalytic Hydrosilylation of Benzonitrile at 70 °C (Table 5). To a mixture of $HSiEt_3$ (0.35 mL, 2.2 mmol) and benzonitrile (0.1 mL, 0.97 mmol) was added a solution of the iridium precatalyst ([**3a**][$BArF_{24}$], 6.7 mg; [**3b**][$BArF_{24}$], 6.8 mg; [**3c**]-

DOI: 10.1021/acs.organomet.7b00749
Organometallics XXXX, XXX, XXX−XXX

[$BArF_{24}$], 7.0 mg; [**3a**][$BArF_{20}$], 5.8 mg; [**3b**][$BArF_{20}$], 5.9 mg, 4.8 μmol; 0.5 mol % relative to benzonitrile) in CH_2Cl_2 (0.5 mL). The reaction mixture was heated at 70 °C for 24 h, after which tri-*tert*-butylbenzene was added as internal NMR standard. An aliquot from this solution was taken and mixed with C_6D_6 for further NMR analysis.

Procedure for the Catalytic Hydrosilylation of Acetophenone at Room Temperature (Table 6). To a mixture of $HSiEt_3$ (0.15 mL, 0.94 mmol) and acetophenone (0.1 mL, 0.86 mmol) was added a solution of the iridium precatalyst ([**3a**][$BArF_{24}$], 1.2 mg; [**3b**][$BArF_{24}$], 1.2 mg; [**3c**][$BArF_{24}$], 1.3 mg; [**3a**][$BArF_{20}$], 1.0 mg; [**3b**][$BArF_{20}$], 1.1 mg, 8.6 μmol; 0.1 mol % relative to acetophenone) in CH_2Cl_2 (0.5 mL). The reaction was allowed to run at room temperature for 30 min, after which tri-*tert*-butylbenzene was added as internal NMR standard. An aliquot of this solution was removed and mixed with C_6D_6 for further NMR analysis.

General Procedure for the Study of the Effect of the Nature of the Counteranion of [3b]$^+$ on the Double Hydrosilylation of Benzonitrile with $HSiEt_3$ (Table 7). All of the reactions were conducted for 24 h at 70 °C following the general procedure 2 described above (Table 4): benzonitrile (0.1 mL, 0.97 mmol), $HSiEt_3$ (0.35 mL, 2.13 mmol), precatalyst (9.7 μmol, 1 mol %), CH_2Cl_2 (0.5 mL).

General Procedure for the Catalytic Hydrosilylation of Nitriles (Scheme 7). To a mixture of silane (1.1−8.8 equiv) and nitrile (1.0 equiv) was added a solution of the precatalyst in CH_2Cl_2 (0.5 mL). The reaction was allowed to take place upon heating at 70 °C for 24 h, after which tri-*tert*-butylbenzene was added as internal NMR standard. An aliquot from this solution was taken and mixed with C_6D_6 for NMR analysis. Further details are provided in the Supporting Information, which include the conditions used for each catalytic run, characterization data of new products, and assigned ^1H NMR spectra of all products.

General Procedure for Competition Experiments (eqs 4 and 5). In a J. Young NMR sample tube was placed an equimolar ratio of the two substrates (benzaldehyde [2.13 or 0.426 mmol], acetophenone [2.13 mmol], or benzonitrile [0.426 mmol] and $HSiEt_3$ (2.13 or 0.426 mmol). Then a solution of [**3b**][$BArF_{24}$] (2.13 μmol, 0.1−0.5 mol % relative to substrate) in CH_2Cl_2 (0.5 mL) was added. The reaction was allowed to run at room temperature for a given time, after which a small aliquot was removed, mixed with a solution of tri-*tert*-butylbenzene in C_6D_6 (∼0.2 mL) used as internal NMR standard, and analyzed by NMR spectroscopy.

General Procedure for the Catalytic Hydrosilylation of Carbonyls. See the Supporting Information for substrate scope. To a mixture of silane (1.1−4.0 equiv) and carbonyl (1.0 equiv) substrates was added a solution of the precatalyst in 0.5 mL of CH_2Cl_2. The reaction was allowed to take place at room temperature for a given time, after which tri-*tert*-butylbenzene was added as internal NMR standard. An aliquot from this solution was taken and mixed with C_6D_6 for NMR analysis. Further details are provided in the Supporting Information, which include the conditions used for each catalytic run, ^1H NMR data of new products, and assigned ^1H NMR spectra of all products.

■ ASSOCIATED CONTENT

Supporting Information

The Supporting Information is available free of charge on the ACS Publications website at DOI: 10.1021/acs.organomet.7b00749.

Extensive experimental, structural, and computational details (PDF)

Cartesian coordinates for the calculated structures (XYZ)

Accession Codes

CCDC 1578556−1578565 contain the supplementary crystallographic data for this paper. These data can be obtained free of charge via www.ccdc.cam.ac.uk/data_request/cif, or by emailing data_request@ccdc.cam.ac.uk, or by contacting The Cambridge Crystallographic Data Centre, 12 Union Road, Cambridge CB2 1EZ, UK; fax: +44 1223 336033.

■ AUTHOR INFORMATION

Corresponding Author

*J.-P.D.: e-mail, djukic@unistra.fr; ph, +33(0)3 68 85 15 23.

ORCID

Mustapha Hamdaoui: 0000-0002-2486-7261

Jean-Pierre Djukic: 0000-0003-3196-4921

Notes

The authors declare no competing financial interest.

■ ACKNOWLEDGMENTS

The authors thank the CNRS, the Agence Nationale de la Recherche (ANR) project COCOORDCHEM, the LABEX "Chimie des Systèmes Complexes", and the University of Strasbourg for funding. The authors gratefully thank Lydia Karmazin and Corinne Bailly for the crystallographic resolution of the structures disclosed therein.

■ REFERENCES

(1) (a) Martin, S. F. *Pure Appl. Chem.* **2009**, *81*, 195−204. (b) Lawrence, S. A. *Amines: synthesis, properties, and applications*; Cambridge University Press: Cambridge, U.K., 2004.

(2) Das, S.; Zhou, S.; Addis, D.; Enthaler, S.; Junge, K.; Beller, M. *Top. Catal.* **2010**, *53*, 979.

(3) Amundsen, L. H.; Nelson, L. S. *J. Am. Chem. Soc.* **1951**, *73*, 242−244.

(4) (a) Bagal, D. B.; Bhanage, B. M. *Adv. Synth. Catal.* **2015**, *357*, 883−900. (b) Gomez, S.; Peters, J. A.; Maschmeyer, T. *Adv. Synth. Catal.* **2002**, *344*, 1037−1057. (c) Tokmic, K.; Jackson, B. J.; Salazar, A.; Woods, T. J.; Fout, A. R. *J. Am. Chem. Soc.* **2017**, *139*, 13554−13561. (d) Mukherjee, A.; Srimani, D.; Ben-David, Y.; Milstein, D. *ChemCatChem* **2017**, *9*, 559−563. (e) Saito, Y.; Ishitani, H.; Ueno, M.; Kobayashi, S. *ChemistryOpen* **2017**, *6*, 211−215. (f) Bornschein, C.; Werkmeister, S.; Wendt, B.; Jiao, H.; Alberico, E.; Baumann, W.; Junge, H.; Junge, K.; Beller, M. *Nat. Commun.* **2014**, *5*, 4111.

(5) Luo, Y.-R. *Comprehensive Handbook of Chemical Bond Energies*; CRC Press: Boca Raton, FL, 2007.

(6) Calas, R.; Frainnet, E.; Bazouin, A. *C.R. Acad. Sci.* **1961**, *252*, 420−422.

(7) Murai, T.; Sakane, T.; Kato, S. *Tetrahedron Lett.* **1985**, *26*, 5145−5148.

(8) Cabrita, I.; Fernandes, A. C. *Tetrahedron* **2011**, *67*, 8183−8186.

(9) (a) Huckaba, A. J.; Hollis, T. K.; Reilly, S. W. *Organometallics* **2013**, *32*, 6248−6256. (b) Itagaki, S.; Sunaba, H.; Kamata, K.; Yamaguchi, K.; Mizuno, N. *Chem. Lett.* **2013**, *42*, 980−982. (c) Campos, J.; Rubio, M.; Esqueda, A. C.; Carmona, E. *J. Labelled Compd. Radiopharm.* **2012**, *55*, 29−38. (d) Caporusso, A. M.; Panziera, N.; Pertici, P.; Pitzalis, E.; Salvadori, P.; Vitulli, G.; Martra, G. *J. Mol. Catal. A: Chem.* **1999**, *150*, 275−285.

(10) Gutsulyak, D. V.; Nikonov, G. I. *Angew. Chem., Int. Ed.* **2010**, *49*, 7553−7556.

(11) (a) Rit, A.; Zanardi, A.; Spaniol, T. P.; Maron, L.; Okuda, J. *Angew. Chem., Int. Ed.* **2014**, *53*, 13273−13277. (b) Boone, C.; Korobkov, I.; Nikonov, G. I. *ACS Catal.* **2013**, *3*, 2336−2340.

(12) Wübbolt, S.; Maji, M. S.; Irran, E.; Oestreich, M. *Chem. - Eur. J.* **2017**, *23*, 6213−6219.

(13) Ito, M.; Itazaki, M.; Nakazawa, H. *ChemCatChem* **2016**, *8*, 3323−3325.

(14) Gandhamsetty, N.; Jeong, J.; Park, J.; Park, S.; Chang, S. *J. Org. Chem.* **2015**, *80*, 7281−7287.

(15) Pérez, M.; Qu, Z.-W.; Caputo, C. B.; Podgorny, V.; Hounjet, L. J.; Hansen, A.; Dobrovetsky, R.; Grimme, S.; Stephan, D. W. *Chem. - Eur. J.* **2015**, *21*, 6491−6500.

DOI: 10.1021/acs.organomet.7b00749
Organometallics XXXX, XXX, XXX−XXX

(16) Bornschein, C.; Werkmeister, S.; Junge, K.; Beller, M. *New J. Chem.* **2013**, *37*, 2061.
(17) Klei, S. R.; Tilley, T. D.; Bergman, R. G. *Organometallics* **2002**, *21*, 4648−4661.
(18) (a) Fogg, D. E.; dos Santos, E. N. *Coord. Chem. Rev.* **2004**, *248*, 2365−2379. (b) Shindoh, N.; Takemoto, Y.; Takasu, K. *Chem. - Eur. J.* **2009**, *15*, 12168−12179.
(19) (a) Iali, W.; Paglia, F. L.; Goff, X.-F. L.; Sredojevic, D.; Pfeffer, M.; Djukic, J.-P. *Chem. Commun.* **2012**, *48*, 10310−10312. (b) Hamdaoui, M.; Ney, M.; Sarda, V.; Karmazin, L.; Bailly, C.; Sieffert, N.; Dohm, S.; Hansen, A.; Grimme, S.; Djukic, J.-P. *Organometallics* **2016**, *35*, 2207−2223.
(20) (a) Corre, Y.; Rysak, V.; Trivelli, X.; Agbossou-Niedercorn, F.; Michon, C. *Eur. J. Org. Chem.* **2017**, *2017*, 4820−4826. (b) Corre, Y.; Trivelli, X.; Capet, F.; Djukic, J.-P.; Agbossou-Niedercorn, F.; Michon, C. *ChemCatChem* **2017**, *9*, 2009−2017. (c) Corre, Y.; Rysak, V.; Capet, F.; Djukic, J.-P.; Agbossou-Niedercorn, F.; Michon, C. *Chem. - Eur. J.* **2016**, *22*, 14036−14041. (d) Corre, Y.; Werle, C.; Brelot-Karmazin, L.; Djukic, J.-P.; Agbossou-Niedercorn, F.; Michon, C. *J. Mol. Catal. A: Chem.* **2016**, *423*, 256−263. (e) Michon, C.; MacIntyre, K.; Corre, Y.; Agbossou-Niedercorn, F. *ChemCatChem* **2016**, *8*, 1755−1762.
(21) (a) Green, M. L. H. *J. Organomet. Chem.* **1995**, *500*, 127−148. (b) Green, M. L. H.; Parkin, G. *Dalton Trans.* **2016**, *45*, 18784−18795. (c) Green, M. L. H.; Parkin, G. *J. Chem. Educ.* **2014**, *91*, 807−816. (d) Green, J. C.; Green, M. L. H.; Parkin, G. *Chem. Commun.* **2012**, *48*, 11481−11503.
(22) Ho Binh, D.; Milovanovic, M.; Puertes-Mico, J.; Hamdaoui, M.; Zaric, S. D.; Djukic, J.-P. *Chem. - Eur. J.* **2017**, DOI: 10.1002/chem.201703373.
(23) Lipke, M. C.; Liberman-Martin, A. L.; Tilley, T. D. *Angew. Chem., Int. Ed.* **2017**, *56*, 2260−2294.
(24) (a) Li, L.; Brennessel, W. W.; Jones, W. D. *J. Am. Chem. Soc.* **2008**, *130*, 12414−12419. (b) Scheeren, C.; Maasarani, F.; Hijazi, A.; Djukic, J.-P.; Pfeffer, M.; Zaric, S. D.; Le Goff, X.-F.; Ricard, L. *Organometallics* **2007**, *26*, 3336−3345. (c) Park-Gehrke, L. S.; Freudenthal, J.; Kaminsky, W.; DiPasquale, A. G.; Mayer, J. M. *Dalton Trans.* **2009**, 1972−1983.
(25) (a) Toennemann, J.; Risse, J.; Grote, Z.; Scopelliti, R.; Severin, K. *Eur. J. Inorg. Chem.* **2013**, *2013*, 4558−4562. (b) White, C.; Yates, A.; Maitlis, P. M.; Heinekey, D. M. *Inorg. Synth.* **1992**, *29*, 228−234.
(26) Fulmer, G. R.; Miller, A. J. M.; Sherden, N. H.; Gottlieb, H. E.; Nudelman, A.; Stoltz, B. M.; Bercaw, J. E.; Goldberg, K. I. *Organometallics* **2010**, *29*, 2176−2179.
(27) (a) Yang, Y. F.; Chung, L. W.; Zhang, X.; Houk, K. N.; Wu, Y. D. *J. Org. Chem.* **2014**, *79*, 8856−8864. (b) Khalimon, A. Y.; Shirobokov, O. G.; Peterson, E.; Simionescu, R.; Kuzmina, L. G.; Howard, J. A. K.; Nikonov, G. I. *Inorg. Chem.* **2012**, *51*, 4300−4313.
(28) (a) Komuro, T.; Begum, R.; Ono, R.; Tobita, H. *Dalt. Trans.* **2011**, *40*, 2348−2357. (b) Zhang, X.-H.; Chung, L. W.; Lin, Z.; Wu, Y.-D. *J. Org. Chem.* **2008**, *73*, 820−829. (c) Watanabe, T.; Hashimoto, H.; Tobita, H. *J. Am. Chem. Soc.* **2006**, *128*, 2176−2177.
(29) Gutsulyak, D. V.; Vyboishchikov, S. F.; Nikonov, G. I. *J. Am. Chem. Soc.* **2010**, *132*, 5950−5951.
(30) Hu, Y.; Li, L.; Shaw, A. P.; Norton, J. R.; Sattler, W.; Rong, Y. *Organometallics* **2012**, *31*, 5058−5064.
(31) (a) Ngo, A. H.; Ibanez, M.; Do, L. H. *ACS Catal.* **2016**, *6*, 2637−2641. (b) Turlington, C. R.; Harrison, D. P.; White, P. S.; Brookhart, M.; Templeton, J. L. *Inorg. Chem.* **2013**, *52*, 11351−11360. (c) Hu, Y.; Li, L.; Shaw, A. P.; Norton, J. R.; Sattler, W.; Rong, Y. *Organometallics* **2012**, *31*, 5058−5064.
(32) (a) Muether, K.; Mohr, J.; Oestreich, M. *Organometallics* **2013**, *32*, 6643−6646. (b) Klare, H. F. T.; Oestreich, M. *Dalton Trans.* **2010**, *39*, 9176−9184.
(33) (a) Bochkarev, M. N.; Balashova, T. V.; Maleev, A. A.; Fagin, A. A.; Fukin, G. K.; Baranov, E. V. *Inorg. Chim. Acta* **2007**, *360*, 2368−2378. (b) Balashova, T. V.; Khoroshenkov, G. V.; Kusyaev, D. M.; Eremenko, I. L.; Aleksandrov, G. G.; Fukin, G. K.; Bochkarev, M. N. *Russ. Chem. Bull.* **2004**, *53*, 825−829. (c) Forsberg, J. H.; Spaziano, V. T.; Balasubramanian, T. M.; Liu, G. K.; Kinsley, S. A.; Duckworth, C. A.; Poteruca, J. J.; Brown, P. S.; Miller, J. L. *J. Org. Chem.* **1987**, *52*, 1017−1021.
(34) (a) te Velde, G.; Bickelhaupt, F. M.; Baerends, E. J.; Fonseca Guerra, C.; van Gisbergen, S. J. A.; Snijders, J. G.; Ziegler, T. *J. Comput. Chem.* **2001**, *22*, 931−967. (b) *ADFview*; SCM, Theoretical Chemistry, Vrije Universiteit, Amsterdam, The Netherlands, 2016.
(35) Steinmann, S. N.; Corminboeuf, C. *J. Chem. Theory Comput.* **2011**, *7*, 3567−3577.
(36) Popelier, P. L. A. *Coord. Chem. Rev.* **2000**, *197*, 169−189.
(37) Bader, R. F. W. In *Atoms in Molecules: A Quantum Theory*; Clarendon: Oxford, U.K, 1990.
(38) Wiberg, K. B. *Tetrahedron* **1968**, *24*, 1083−1096.
(39) (a) Grossekappenberg, H.; Reissmann, M.; Schmidtmann, M.; Mueller, T. *Organometallics* **2015**, *34*, 4952−4958. (b) Gaspar, P. P. *Science* **2002**, *297*, 785−786. (c) Mueller, T. *Struct. Bonding (Berlin, Ger.)* **2013**, *155*, 107−162.
(40) Nava, M.; Reed, C. A. *Organometallics* **2011**, *30*, 4798−4800.
(41) (a) Hosomi, A.; Miura, K. In *Comprehensive Organometallic Chemistry III*; Crabtree, R. H., Mingos, D. M. P., Eds.; Elsevier: Oxford, U.K., 2007; pp 297−339. (b) Lambert, J. B.; Zhang, S.; Ciro, S. M. *Organometallics* **1994**, *13*, 2430−2443. (c) Kessler, M.; Knapp, C.; Sagawe, V.; Scherer, H.; Uzun, R. *Inorg. Chem.* **2010**, *49*, 5223−5230.
(42) (a) Boberski, W. G.; Allred, A. L. *J. Organomet. Chem.* **1975**, *88*, 65−72. (b) Arshadi, M.; Johnels, D.; Edlund, U.; Ottosson, C.-H.; Cremer, D. *J. Am. Chem. Soc.* **1996**, *118*, 5120−5131.
(43) (a) Lambert, J. B.; Kania, L.; Zhang, S. *Chem. Rev.* **1995**, *95*, 1191−1201. (b) Lambert, J. B.; Zhang, S. *J. Chem. Soc., Chem. Commun.* **1993**, 383−384.
(44) Garcés, K.; Fernández-Alvarez, F. J.; Polo, V.; Lalrempuia, R.; Pérez-Torrente, J. J.; Oro, L. A. *ChemCatChem* **2014**, *6*, 1691−1697.
(45) (a) Haiges, R.; Baxter, A. F.; Goetz, N. R.; Axhausen, J. A.; Soltner, T.; Kornath, A.; Christe, K. O. *Dalt. Trans.* **2016**, *45*, 8494−8499. (b) Reed, C. A. *Acc. Chem. Res.* **2013**, *46*, 2567−2575.
(46) (a) Bahr, S. R.; Boudjouk, P. *J. Am. Chem. Soc.* **1993**, *115*, 4514−4519. (b) Kira, M.; Hino, T.; Sakurai, H. *Chem. Lett.* **1993**, *22*, 153−156.
(47) (a) Reißmann, M.; Schäfer, A.; Jung, S.; Müller, T. *Organometallics* **2013**, *32*, 6736−6744. (b) Herrington, T. J.; Ward, B. J.; Doyle, L. R.; McDermott, J.; White, A. J. P.; Hunt, P. A.; Ashley, A. E. *Chem. Commun.* **2014**, *50*, 12753−12756. (c) Scott, D. J.; Fuchter, M. J.; Ashley, A. E. *Angew. Chem., Int. Ed.* **2014**, *53*, 10218−10222.
(48) Corre, Y.; Rysak, V.; Trivelli, X.; Agbossou-Niedercorn, F.; Michon, C. *Eur. J. Org. Chem.* **2017**, *2017*, 4820−4826.
(49) (a) Noedling, A. R.; Muether, K.; Rohde, V. H. G.; Hilt, G.; Oestreich, M. *Organometallics* **2014**, *33*, 302−308. (b) Kim, K.-C.; Reed, C. A.; Elliott, D. W.; Mueller, L. J.; Tham, F.; Lin, L.; Lambert, J. B. *Science* **2002**, *297*, 825−827. (c) Khalimon, A. Y.; Lin, Z. H.; Simionescu, R.; Vyboishchikov, S. F.; Nikonov, G. I. *Angew. Chem., Int. Ed.* **2007**, *46*, 4530−4533. (d) Hoffmann, S. P.; Kato, T.; Tham, F. S.; Reed, C. A. *Chem. Commun.* **2006**, 767−769.
(50) Davies, D. L.; Al-Duaij, O.; Fawcett, J.; Giardiello, M.; Hilton, S. T.; Russell, D. R. *Dalton Trans.* **2003**, *2*, 4132−4138.
(51) Scott, V. J.; Çelenligil-Çetin, R.; Ozerov, O. V. *J. Am. Chem. Soc.* **2005**, *127*, 2852−2853.
(52) Connelly, S. J.; Kaminsky, W.; Heinekey, D. M. *Organometallics* **2013**, *32*, 7478−7481.
(53) Note that two structures were acquired and resolved for [**4b**][$BArF_{24}$], to which were applied the SQUEEZE procedure to restrain residual electron density pertaining to solvent molecules present within the crystal lattice: i.e., benzene and *n*-hexane molecules respectively. Figure 6 depicts the structure containing unresolved *n*-hexane.

DOI: 10.1021/acs.organomet.7b00749
Organometallics XXXX, XXX, XXX−XXX